UPPSALA
UNIVERSITET

Digital Comprehensive Summaries of Uppsala Dissertations from the Faculty of Science and Technology 1061

Superdiffusive Spin Transport and Ultrafast Magnetization Dynamics

Femtosecond spin transport as the route to ultrafast spintronics

MARCO BATTIATO

ACTA
UNIVERSITATIS
UPSALIENSIS
UPPSALA
2013

ISSN 1651-6214
ISBN 978-91-554-8722-5
urn:nbn:se:uu:diva-205265

Dissertation presented at Uppsala University to be publicly examined in Siegbahnsalen, Lägerhyddsvägen 1, Uppsala, Friday, September 27, 2013 at 13:00 for the degree of Doctor of Philosophy. The examination will be conducted in English.

Abstract
Battiato, M. 2013. Superdiffusive Spin Transport and Ultrafast Magnetization Dynamics: Femtosecond spin transport as the route to ultrafast spintronics. Acta Universitatis Upsaliensis. *Digital Comprehensive Summaries of Uppsala Dissertations from the Faculty of Science and Technology* 1061. 62 pp. Uppsala. ISBN 978-91-554-8722-5.

The debate over the origin of the ultrafast demagnetization has been intensively active for the past 16 years. Several microscopic mechanisms have been proposed but none has managed so far to provide direct and incontrovertible evidences of their validity. In this context I have proposed an approach based on spin dependent electron superdiffusion as the driver of the ultrafast demagnetization.

Excited electrons and holes in the ferromagnetic metal start diffusing after the absorption of the laser photons. Being the material ferromagnetic, the majority and minority spin channels occupy very different bands. It is then not surprising that transport properties are strongly spin dependent. In most of the ferromagnetic metals, majority spin excited electrons have better transport properties than minority ones. The effect is that majority carriers are more efficient in leaving the area irradiated by the laser, triggering a net spin transport.

Recent experimental findings are revolutionising the field by being incompatible with previously proposed models and showing uncontrovertibly the sign of spin superdiffusion.

We have shown that spin diffusing away from a layer undergoing ultrafast demagnetization can be used to create an ultrafast increase of magnetization in a neighboring magnetic layer. We have also shown that optical excitation is not a prerequisite for the ultrafast demagnetization and that excited electrons superdiffusing from a non-magnetic substrate can trigger the demagnetization. Finally we have shown that it is possible to control the time shape of the spin currents created and developed a technique to detect directly spin currents in a contact-less way.

The impact of these new discoveries goes beyond the solution of the mystery of ultrafast demagnetization. It shows how spin information can be, not only manipulated, as shown 16 years ago, but most importantly transferred at unprecedented speeds. This new discovery lays the basis for a full femtosecond spintronics.

Keywords: Ultrafast magnetisation dynamics, anomalous diffusion, femtosecond dynamics, magnetism

Marco Battiato, Uppsala University, Department of Physics and Astronomy, Materials Theory, Box 516, SE-751 20 Uppsala, Sweden.

ISSN 1651-6214
ISBN 978-91-554-8722-5
urn:nbn:se:uu:diva-205265 (http://urn.kb.se/resolve?urn=urn:nbn:se:uu:diva-205265)

List of papers

This thesis is based on the following papers, which are referred to in the text by their Roman numerals.

I **Superdiffusive Spin Transport as a Mechanism of Ultrafast Demagnetization**
M. Battiato, K. Carva, and P.M. Oppeneer
Phys. Rev. Lett. **105**, 027203 (2010).

II **Theory of laser-induced ultrafast superdiffusive spin transport in layered heterostructures**
M. Battiato, K. Carva, and P.M. Oppeneer
Phys. Rev. B 86, 024404 (2012).

III **Ultrafast magnetization enhancement in metallic multilayers driven by superdiffusive spin current**
D. Rudolf,* C. La-O-Vorakiat,* M. Battiato,* R. Adam, J. M. Shaw, E. Turgut, P. Maldonado, S. Mathias, P. Grychtol, H. T. Nembach, T. J. Silva, M. Aeschlimann, H. C. Kapteyn, M. M. Murnane, C. M. Schneider, and P. M. Oppeneer
Nature Comm. **3**, 1037 (2012)

IV **Ultrafast spin transport as key to femtosecond demagnetization**
A. Eschenlohr,* M. Battiato,* P. Maldonado, N. Pontius, T. Kachel, K. Holldack, R. Mitzner, A. Föhlisch, P. M. Oppeneer, and C. Stamm
Nature Mater. **12**, 332 (2013).

V **Engineering ultrafast spin currents and terahertz transients by magnetic heterostructures**
T. Kampfrath, M. Battiato, P. Maldonado, G. Eilers, J. Nötzold, I. Radu, F. Freimuth, Y. Mokrousov, S. Blügel, M. Wolf, P. M. Oppeneer, and M. Münzenberg
Nature Nanotechnol. **8**, 256 (2013)

* All these authors contributed equally

Reprints were made with permission from the publishers.

Publications not included in this thesis

- Comment: **Is the controversy over femtosecond magneto-optics really solved?**
  K. Carva, M. Battiato, and P.M. Oppeneer
  Nature Phys. **7**, 665 (2011).

- **Beyond linear response theory for intensive light-matter interactions: order formalism and ultrafast transient dynamics.**
  M. Battiato, G. Barbalinardo, K. Carva, and P. M. Oppeneer.
  Phys. Rev. B **85**, 045117 (2012).

- **Ab initio investigation of the Elliott-Yafet electron-phonon mechanism in laser-induced ultrafast demagnetization**
  K. Carva, M. Battiato, and P.M. Oppeneer
  Phys. Rev. Lett. **107**, 207201 (2011).

- **Ab initio theory of electron-phonon mediated ultrafast spin relaxation of laser-excited hot electrons in transition-metal ferromagnets**
  K. Carva, M. Battiato, D. Legut, and P.M. Oppeneer
  Phys. Rev. B. **87**, 184425 (2013).

- **Quantum theory of the inverse Faraday effect: framework for material specific *ab initio* calculations**
  M. Battiato, G. Barbalinardo, and P. M. Oppeneer
  manuscript

Contents

Preface

The reader who will quickly leaf through the pages of this thesis will notice that there is a lot of text, quite a few pictures but not many lenghty equations. This might seem strange for a theoretical thesis, but it is due to the fact that I spent most of the effort trying to give intuitive physical picture of the mechanisms and their effects and consequences. I tried to avoid all technical problems (that were definitely more than few) related to the mathematics and numerics. Most of the technical details are anyhow available in the reprints of the papers attached at the end of the thesis. The numeric, on the other hand, is not treated either in this thesis or in the articles.

The first reason behind this choice is that, in spite of the importance of the technical part of the job I conducted during my PhD, I believe that the most important contribution I gave to the field with my work has been the physical understanding of the effect of transport in femtosecond dynamics and the description of the physical mechanisms.

The second is that my aim has been also to write a thesis that can introduce other scientists to the topic. I definitely do not want to aim it at theoreticians only, but to the broadest audience possible. I therefore tried to always provide as intuitive as possible pictures of the mechanisms proposed.

Thirdly, I have also chosen a very descriptive approach because I personally believe that, even if technical qualities are fundamental to a scientist, if they are not led by physical intuition they cannot be used to tackle front line physical problems.

Finally I find technical problems fun to solve, but really, really boring to read about.

Marco

1. Introduction

The development of the femtosecond laser technology created the possibility of investigating the dynamics of quantum systems in unprecedented timescales. Laser pulses can now be shrunk down to few tens of fs. Systems irradiated with these optical pulses can be driven into strongly excited states and trigger dynamics before the electrons thermalise. Furthermore the development of the pump-and-probe technique allowed a very precise analysis of the triggered dynamics. The great efficiency and the relatively low cost of this technique quickly elevated it to the most popular way to address fs dynamics. The spectrum of important discoveries is extremely wide. One of the most important has been done in 1996 by Beaurepaire *et al.* [2]. They showed first that magneto-optical probing techniques could be adapted to fs dynamics. But the unexpected discovery was that the magnetization of a ferromagnetic Ni film quenched within a sub-picosecond timescale after a fs laser irradiation. To understand the impact of the discovery one should compare those dynamics with the fact that modern magnetic hard drives achieve the switch of a magnetic bit within 1ns. In R&D facilities the switching can be ten times as fast. Ultrafast laser induced magnetization dynamics are al least 3 orders of magnitude faster. The promise of ultrafast magnetic recording technology has attracted a vast interest towards the topic.

Nonetheless, in spite of more than fifteen years of intense study, the microscopical mechanism of the ultrafast demagnetization has remained elusive and not understood. The greatest theoretical challenge is to explain how and where the spin angular momentum has been transferred, since it has to be removed from the spin system in order to achieve the demagnetization. In a very famous experiment Einstein and de Haas showed the relationship between magnetism, angular momentum and spin. They hanged a bulky ferromagnet from a thin wire and observed that, upon change of its magnetization, the magnet started spinning. What had happened was that the reduction of the magnetization of the ferromagnet caused a misalignment of the atomic spin moments leading to a net reduction of the total spin moment. To allow that, spin angular momentum had to be removed from the spin system. The conservation of angular momentum enforces that the angular momentum cannot be destroyed but only transferred. Einstein and de Haas showed that the spin angular momentum was eventually transferred to the phonon system or equivalently to the lattice.

Since then, the transfer of angular momentum that allowed for macroscopic magnetization changes has been widely studied and this mechanism was considered to be well understood, the timescale of these dynamics being of tens

of picoseconds and slower. Unexpectedly the experiment by Beaurepaire *et al.* showed that macroscopic changes of magnetization could be achieved in as short as few hundreds of fs.

A strong debate was born around the nature of the dissipation channel that would allow the spin angular momentum to be removed from the spin system at such unprecedented speed. Many microscopic mechanisms have been proposed, e.g. the Elliott-Yafet electron-phonon spin-flip scattering driven either by the temperature difference between the electronic system and the lattice [23, 22, 12] or by a hot-electron-driven enhancement of spin-lattice coupling [51], electron-magnon [5] or electron-electron scattering [25], or relativistic laser-field induced spin-flips [3]. In spite of several arguments and experiments supporting each of the aforementioned mechanism, none managed so far to provide incontrovertible evidences and predict all the main characteristics of the ultrafast demagnetization. They are at the present still under debate.

In Paper I I proposed a different approach. I abandoned the idea of ultrafast enhancement of known slow spin-dissipation channel and assumed spin-flip events to be rare in this timescale, as the knowledge developed before the discovery of ultrafast demagnetization predicts. In absence of spin flip events, the demagnetization is proposed to be driven by a magnetization flux away from the ferromagnetic film, caused by the spin dependent diffusion of laser excited non-equilibrium electrons. The specific diffusion regime of electrons in the femtosecond timescale required a modelling based on superdiffusive kinematic description.

In ferromagnetic materials, transport properties of both electrons excited above the Fermi energy and holes below are strongly spin dependent. In particular spin majority electrons have, in the case of ferromagnetic transition metals and most of their alloys, a strongly higher mobility than minority ones. After the excitation by a fs laser, electrons from d-states below the Fermi energy are excited to sp-states above the Fermi energy forming electron-hole pairs. Majority spins non-equilibrium electrons have now high velocities of around 1nm/fs and undergo a very efficient diffusion process away from the optically excited area leading to a net demagnetization of that region. The demagnetization process perdures as long as the electronic system does not reach an electronic thermalisation. The total magnetization of the sample is not changed but, when optically probing the area that has been excited, a demagnetization will be measured.

The spin superdiffusion model [Papers I and II] was able to predict the amplitude and the timescale of the demagnetization of a typical demagnetization experiment. Moreover the model is able to explain the existence of the ultrafast demagnetization in ferromagnetic metals while, instead, in dielectrics is much slower [20, 33] and the saturation of the demagnetization at high fluences [20].

A first hint that direct spin transfer could play a role in the ultrafast demagnetization was presented by Malinowski *et al.* [29]. In spite of that experiment

soon after the contribution was disregarded as a side effect. But after the theoretical prediction in Paper I, recent experimental evidences have been provided that strongly support the proposed model. Melnikov *et al.* [32] showed how a magnetic signal is measured on the gold surface of a Fe/Au sample after a fs irradiation of the Fe film, providing a strong evidence supporting the presence of spin transport. More recently it has been shown how spin transport strongly influences magnetization dynamics in films with lateral patterns of antiferromagnetically aligned magnetic domains [48, 34]. It is also been proposed that spin transport plays an important role in the all-optical switching of GdFeCo films [16].

In Paper IV we have proposed that laser irradiation is not a prerequisite to the ultrafast demagnetization, and that electrons superdiffusing from a neighbouring layer can induce it as efficiently. The spin superdiffusion model is in excellent qualitative and good quantitative agreement with the experiments.

We have also been able to predict and give experimental evidences in Paper III of a completely new phenomenon: an ultrafast magnetization *enhancement*. We have triggered spin superdiffusion from a ferromagnet Ni film into a ferromagnetic Fe film. The spin polarisation of the magnetization flux was defined by the magnetization orientation in Ni and it has been used to affect the magnetization of the Fe layer. In the case the two layers had antiparallel alignment the Fe underwent an ultrafast demagnetization. But, in sharp contradiction with all the other proposed models of the ultrafast demagnetization, in the case parallel magnetizations in the two layers, an ultrafast *increase* of the magnetization in Fe has been observed. This shows that magnetization is ejected from the Ni film during the ultrafast demagnetization and injected in Fe.

The concept of spin superdiffusion has been also used in Paper V to build a broadband THz emitter and show the possibility to control spin currents with the aim of creating fs spintronic devices. We have also showed that the spin superdiffusion model can give accurate predictions of the shape of fs laser-generated spin currents and developed a technique to measure THz spin currents in a contactless manner.

Nonetheless the research in the field is not concluded yet. Strong evidences show the dominant role of spin superdiffusion in the process of ultrafast demagnetization, but it is still unclear if this mechanism is the only driver or other effects contribute as well or might be dominant in different configurations. Even though a big step forward has been made in the understanding of the microscopic mechanism of the ultrafast demagnetization, the most important implication of these new discoveries is the drastic change of the potential related to the field of ultrafast magnetization dynamics. Before the importance of transport processes was discovered, the magnetization change was considered a local process. This meant that what could be expected from technological applications was to modify locally the magnetic moment with a laser in ultrafast magneto hard-drives. The discovery of ultrafast spin su-

perdiffusion proves the possibility of, not only, modifying the magnetization in unprecedented ways, but more importantly the possibility of transporting spin information in bunches few hundreds of fs wide with speed of 1nm/fs. This paves the road to the development of real THz electronics manipulating spin or femtosecond spintronics.

2. Experimental and theoretical background

The field of magnetization dynamics is extremely vast. It spans over a wide range on timescales and requires a variety of modelling tools. Precessional dynamics of magnetization, domain wall motion, vortex creation and magnon propagation are examples of relevant processes in the pico to nanosecond timescales. Landau-Lifshitz (LL), Landau-Lifshitz-Gilbert (LLG), Landau-Lifshitz-Bloch (LLB) equations, supported by *ab initio* calculations of exchange parameters, are examples of very successful descriptions of magnetization dynamics. Micromagnetic simulations access bigger scales with high efficiency and reliability. Given the deep technological relevance of many of these processes, a great degree of effort has been put into driving and controlling them in faster and faster timescales.

However the extension of these technologies in the sub-picosecond region poses very fundamental challenges. For instance it has been shown that magnetization reversal by applied magnetic fields does not occur in a deterministic way for a pulse duration of less than 2.3ps [47]. Moreover the possibility of manipulating the magnetization in less than 1ps was expected to be unachievable. Nonetheless experiments showed that magnetic ordering can be strongly manipulated in as short as few hundreds of fs, but so far the very microscopical origin of many of these phenomena is yet unclear.

Various kinds of dynamics have been observed in ferromagnetic and ferrimagnetic metals and semiconductors[20]. Another phenomenon of a more complex nature and spanning different timescales is the all-optical switching [43]: in a narrow class of metals (like GdFeCo and TbFeCo alloys), a magnetization reversal can be obtained within tens of picoseconds or more.

The field is changing at a very fast pace. New unexpected dynamics have been observed [Paper III] and the importance of transport processes has been highlighted [Papers I, II and IV]. Moreover the idea that all sub-picosecond magnetization dynamics should have been optically driven has been recently disproven [Paper IV].

2.1 Towards the ultrafast demagnetization

The physics of sub-picosecond dynamics became accessible when pulsed femtosecond lasers and the pump and probe technique were developed in the late 1980s. In a typical pump-and-probe experiment the fs laser pulse is split into an intense pump pulse and a weaker probe pulse. The pump pulse is sent to

the sample to create the excitation needed to trigger the dynamics under study. Conversely the probe pulse will be used to test the response of the system by measuring how the probe pulse is affected by the sample. Several standard probing techniques have been successfully adapted to the fs dynamics. Because of the small time width, the probe pulse interacts with the sample only for a limited time giving an averaged information about the state of the latter only within this time window. This is used to measure the sample response to the pump pulse after a given time. With this aim the probe pulse, before being shone on the sample, is sent to a adjustable delay line, allowing a precise calibration of the position of the probed time window. The experiment is then repeated at different delay times to construct in a stroboscopic way the complete time evolution of the system after the excitation by the pump pulse. It is important to stress here that since the experiment has to be reproduced every time a new point in time has to be measured, the dynamics of the system need to be reproducible and stable, and that it is necessary to bring back the system to the initial condition after every pump and probe snapshot.

This new technique made it possible to analyse the dynamics of a system brought out of equilibrium by an intense short laser pulse. The first pump and probe experiments focused on electron dynamics of simple metals like Au, Ag, Cu by probing both reflectivity [4, 18, 45] and photoemission spectroscopy [14]. The analysis focused mainly on the identification of the timescales of electron thermalisation after the laser excitation [15] and of the regimes of electron transport [18]. Only later the same technique has been applied to magnetic measurement. This led to the discovery of ultrafast demagnetization [2]. Beaurepaire *et al.* pumped a 22nm thick Ni film grown on Al substrate with a 60fs laser pulse at 2eV. By measuring time resolved hysteresis loops of magneto-optical Kerr effect (MOKE) they found a drop of the remanent magnetization of almost 50% within the first picosecond (Fig. 2.1).

After the first observation of the ultrafast demagnetization, several complementary techniques have been employed to study it. The results from Beaurepaire *et al.* were confirmed by second harmonic generation (SHG) measurement [17], even though it was pointed out that both MOKE and SHG measurements could suffer from optical artefacts due to the associated change in reflectivity of the material [36, 24]. Later time- and spin resolved two-photon-photoemission (2PPE) experiments [39, 50] showed strong reduction of the spin polarisation on a sub-picosecond timescale. The use of synchrotron radiation to perform x-ray magnetic circular dichroism (XMCD) allowed element selectivity of ultrafast demagnetization experiments [41]. The further advance of time resolved XMCD spectroscopy allowed, by using sum rules on Ni L_2 and L_3 edges, to measure the reduction of the spin and orbital angular momentum separately [42], giving for the first time an incontrovertible evidence that ultrafast demagnetization is caused by a real decrease of the spin moment. A very recent experimental advancement has been obtained by the application of femtosecond soft x-ray pulses from high-harmonic generation to measure

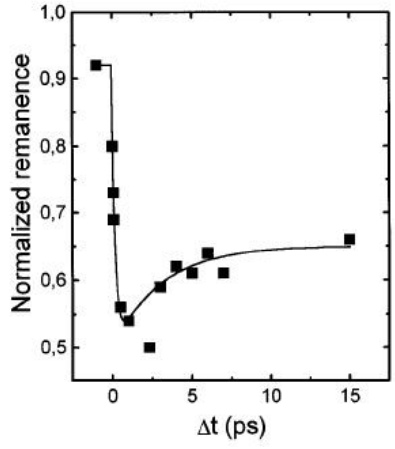

Figure 2.1. Sub-picosecond magneto-optical signal reduction after fs optical pump [2].

transverse magneto-optic Kerr effect (T-MOKE) [27]. The broad spectrum of the XUV allowed a single shot measurement of a T-MOKE spectrum. This meant that it is possible to measure element-specific magnetic signals by single shot with a tabletop setup [28, 31].

More than fifteen years of intense, high quality research have provided a systematic study and characterisation of the ultrafast demagnetization. It is worth stressing that the considerations below will apply to ferromagnets: ferrimagnets and antiferromagnets are more complex materials with more degree of freedom and the possibility to activate more kinds of dynamics compared to simple ferromagnets. The first fundamental feature of the ultrafast demagnetization that became apparent is that it can be observed in all ferromagnetic metals, while in ferromagnetic insulators the demagnetization following a fs laser pulse excitation is orders of magnitude slower [20]. Among the metals, ferromagnetic transition metals have been intensively studied. It has been understood that the ultrafast demagnetization is triggered by the laser pulse but continues even after the laser field has already vanished. In most modern experiments the time width of the laser pulse is usually much shorter than the demagnetization time and the time width of the laser does not seem to affect significantly the demagnetization time. It has also been proven that eventual circular polarisation of light does not play any role [10], nor does the external magnetic field [24]. Another fundamental feature is that the demagnetization increases linearly with the laser fluence (it is quadratic in the electric field), but soon saturates at high fluences [22]. A complete demagnetization in simple ferromagnetic transition metals has never been observed, and the maximum has been around 90% [8].

The demagnetization time instead is strongly material dependent, but even for the same materials, experiments are not always in agreement on the de-

magnetization times. They seem to depend on the amount of demagnetization, the quality and geometry of the sample, other than the material itself. In particular it has been observed that increasing absorbed fluences, and therefore an increasing demagnetization, lead to longer demagnetization time constants [22]. Measured time constants are around 140-200fs for Ni [22], 50-75fs for Fe [5] and 160-240fs for Co [22].

2.2 The mystery of the angular momentum

The main challenge related to the understanding of the microscopic mechanism of the ultrafast demagnetization is finding the channel of dissipation of angular momentum in the femtosecond timescale. Conservation of angular momentum is one of the fundamental conservation laws in physics. It states that in a closed system, angular momentum cannot be created or destroyed.

During the ultrafast demagnetization angular momentum is removed from the spin system. Note that this is regardless the fact whether the demagnetization is caused by an atomic reduction of the spin polarisation or from a randomisation of the orientation of the atomic magnetic moments or even in the disproven scenario in which the magnetic moment of the film simply tilts towards another direction. If any of the cartesian components of the total spin moment of the whole system is changed, the corresponding difference in angular momentum has to be converted into another type of angular momentum or injected into the system from outside.

Photon angular momentum

One external source of angular momentum can be light. Each photon transports one quantum of angular momentum. Upon absorption the electronic system increases its energy by $\hbar\nu$ and its total angular momentum by $\hbar$. The interaction between a photon and an electron can be, with excellent approximation, modelled only by the interaction between the photon electric field and the electron charge. If no relativistic effects are taken into account, the matrix elements between states with different spins are zero and therefore no spin-flip excitations are allowed. But if the spin-orbit (SO) interaction is not negligible in the system, there are no pure spin states and a net spin flip becomes allowed (see Fig. 2.2.a). Nonetheless only a fraction of all the absorption processes will lead to a spin flip and this fraction is in first approximation proportional to the SO interaction.

Zhang *et al.* advanced the hypothesis [52] that ultrafast demagnetization could be caused by direct angular momentum transfer form the photons following the mechanism outlined above. A similar microscopic mechanism [3] has been proposed by Bigot *et al.*, which also takes into account a time-dependent modification of the SO interaction. It is currently under discussion [40, 11] whether the number of photons absorbed in the material are enough

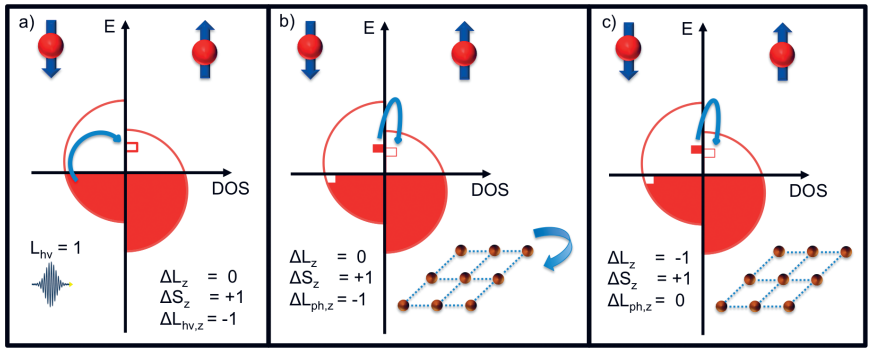

Figure 2.2. Examples of spin-flip events upon interaction between the electronic system and an external one. a) Photon-induced spin-flip: the electron absorbs a photon and has a probability to increase its spin angular momentum instead of its orbital one. b) Phonon-induced spin-flip: the electron emits a phonon with a finite angular momentum and spin flips. c) Phonon-mediated spin-flip: the electron emits a phonon with vanishing angular momentum and spin flips by reducing its own angular momentum

to induce the measured demagnetization. Moreover, according to the model, the demagnetization should be instantaneous and the demagnetization time should be set by the laser pulse length, which is disproved by experiments. Finally the role of the angular momentum brought by the light has been already ruled out [10]. In their experiment, Dall Longa *et al.* analysed the effect of light polarisation on the demagnetization. In particular they showed that the light polarisation had a negligible effect on the amount of demagnetization observed, even in the case of circularly polarised light with angular momentum aligned parallel to the magnetization, where, according to the model above, no demagnetization at all should be observed or at most an increase of magnetization.

Phonon angular momentum

Einstein and de Haas showed how, upon reduction of the magnetization, the spin angular momentum is eventually transferred to the lattice. The microscopical mechanism of this transfer can be imagined as following some intuitive channels, all included in the Elliott-Yafett spin-flip mechanism. In one case (see Fig. 2.2.b) angular momentum is transferred directly from the spin system to the phonon system. In figure the scattering of an excited electron with a phonon has been showed because it allowed for simpler graphic representation, but electrons at the Fermi energy can as well experience an Elliott-Yafett scattering absorbing a phonon. Another possible spin-flip event can be with no transfer of angular momentum to the lattice and simply conversion of orbital angular momentum to spin (see Fig. 2.2.c). A phonon has a defined wavevector, but can be a superposition of several states at defined angular momentum. Henceforth the Elliott-Yafet mechanism can lead to more com-

plex transfers where more than a single quantum is transferred. Nonetheless, equivalently to what pointed out for photon-induced spin-flips, every electron-phonon scattering there is only a small chance, proportional to the SO degree of spin mixing, that an Elliott-Yafet spin-flip can be achieved. Moreover not all the spin-flip events act towards a magnetization reduction. It is then a question whether in as little as few hundreds of femtoseconds there is a sufficient number of net spin-flips via this mechanism.

Koopmans *et al.* proposed [21] the mechanism above as the driver of the ultrafast demagnetization. The model linked the demagnetization time to the Gilbert damping [23, 13], but experiments [49, 35] shown that modifying it in rare-earth doped $Ni_{80}Fe_{20}$ by tuning the doping did not modify the demagnetization time as predicted. Koopmans *et al.* recently proposed [22] a more sophisticated model, called microscopic three temperatures model (M3TM), based on *ab initio* calculated Elliott-Yafet spin-flip probabilities [44]. The model has been able to reproduce some characteristic features of the ultrafast demagnetization in some materials [22], but has not been able yet to provide incontrovertible evidences. It is currently under debate [6]. Essert *et al.* also assert that a rigid band structure, as the one used in the M3TM, will provide too few spin-flip events to explain the ultrafast demagnetization, both in case they are driven by electron-phonon scatterings and any other kind of scattering. They conclude that a correct description of the dynamical changes of the band structure is necessary. Wietstruk *et al.* support the idea that ultrafast demagnetization is driven by electron-phonon spin flips increased by the dynamical enhancement of the spin-lattice coupling [51].

3. Superdiffusive spin transport

The direct effect of the femtosecond laser pulse on a ferromagnetic metal, as shown above, is still a topic under debate. The issue of establishing also how the probe itself interacts with the material and what information can be extracted, together with the problem of artefacts coming from partial temporal superposition of pump and probe are still under open discussion. Nonetheless in this chapter the pump will be considered only up to the second order and will modify the system only through absorption. I will therefore focus on the longer timescale of hundreds of femtoseconds up to picoseconds .

Many extremely important effects are active in this timescale. Laser excited electrons will undergo thermalisation by electron-electron scatterings, while heat (or energy) will be transferred to the lattice via electron-phonon scatterings. Spin-flip events can happen during one of those scatterings, and magnons can be generated and propagate.

At the same time, in metals, the excitons created after the laser absorption can move within the material. This effect will play a fundamental role for ultrafast magnetization dynamics. I will show in the following pages how the sub-picosecond diffusion of excitons cannot be neglected in the timescale of the electron thermalisation. I will show how standard approaches cannot describe with acceptable approximation this phenomenon and that a new description is required. I will finally highlight how the spin dependent transport properties in a ferromagnet lead to spin diffusion and how the latter is one of the driver, possibly the only one, of the ultrafast demagnetization. The present chapter will mainly focus on the theoretical description, while the following one will address quantitative predictions and comparison with experiments.

In Sec. 3.1 I will start by focusing on a simpler effect: the femtosecond energy diffusion in a non-magnetic material. In Sec. 3.2 I will introduce a semiclassical model to describe exciton diffusion in the sub-picosecond timescale, and extensively describe its physical implications. After that, in Sec. 3.3 I will show how in a ferromagnetic metal strongly spin dependent transport properties lead to a net spin diffusion. Finally in Sec. 3.4 I will analyse and discuss other dynamics that can take place in the timescale of hundreds of femtoseconds.

3.1 Femtosecond exciton diffusion in metals

Heat transport in insulators is mainly due to the propagation of lattice vibrations. In metals, however, a big contribution is given by the electrons transport.

If we heat up one side of a metal bar hot electrons diffuse towards the cold side while cold electrons do the same towards the hot one. A very similar effect happens in the femtosecond timescale.

Optical light has usually very short penetration depths in metals (of the order of few tens of nm). Therefore shining a femtosecond laser pulse on a metallic film acts as a very fast heating of a very small region up to a few laser penetration depths. Electrons close to the surface absorb the energy corresponding to the laser frequency and start diffusing. While they travel, they carry their energy (and, as we will see below, other quantities as well). In spite of the fact that the process described above seems extremely similar to thermal heat transport, the peculiar characteristics of the electron diffusion in the femtosecond timescale need to be addressed carefully and will require a more sophisticated description.

In the following I will give first an intuitive description of the process. The semiclassical analogy will be pushed sometimes to a level that might turn up someone's nose. At this stage, the main aim is only to provide an overall picture of what we aim at describing. A hint of the mathematics behind the model will be given in Sec.3.2, while a closer look at the quantum mechanical aspects will be given in Sec. 3.3.

Finally the assumption of small excitation underlines the whole treatment. The effect of finite excitation will be addressed further below in Sec. 3.4.1. In the case of small excitations in metal a single electron excitation picture provides a very good approximated description of the many-body exciton state. Within the same approximation a rigid band structure after the excitation gives the same order of accuracy.

3.1.1 Introduction to excited electron and hole diffusion

As an example I will use a simplified band structure of a metal with d-states crossing the Fermi energy, for the similarity of its density of states (Fig 3.1.a) with the one of transition metal ferromagnets. At thermal equilibrium all the states below the Fermi energy are occupied while the states above are empty (see Fig 3.1.a). We can neglect the effect of the initial temperature since thermal energies are negligible compared to the typical photon energy of the laser excitation of around 1-3 eV. During the laser excitation, photons are absorbed in the metal. Upon the absorption of one photon, an electron from a state below the Fermi level is excited to another empty states above the Fermi energy.

The exciton's shape will be the one of a wavepacket. In order to treat a wavepacket as a semiclassical particle, it needs to be fairly localised in space. However this implies that it extends in the reciprocal space and consequently in energy. Nonetheless if the wavepacket would span a too wide range of energy, the description of the motion will be non semiclassical. Therefore, given the required spatial localisation, the energies covered by the wavepacket have

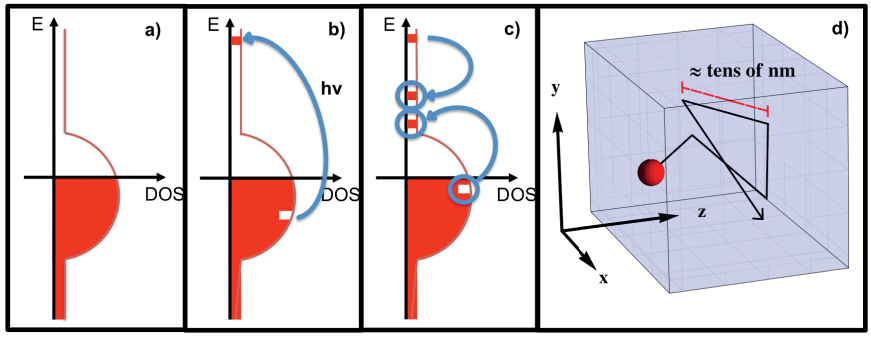

Figure 3.1. a) Schematic density of states of material with d-bands crossing the Fermi energy. b) Single particle picture of excitation induced by laser absorption. c) Single particle picture of electron-electron scattering. d) Schematic 3D picture of excited electron diffusion after laser excitation.

to be close enough to ensure that the transport properties vary little along this energy range. In one dimension a wavepacket covering $1/n$ of the Brillouin zone extends for about n lattice parameters [1]. To achieve a spatial localisation of 1-2 nm in the transition metals under study, it is necessary to cover around 1/10 of the Brillouin zone. In case of d-bands the energy range associated to such localisation in the reciprocal space is very small. In case of more mobile bands the energy range can become bigger, but on the other hand the transport properties vary more slowly. For these reasons the description of the wavepacket using the position of the centre of mass and the median energy remains a good approximation.

From now on I will refer to the part of the exciton described by the wavepacket above the Fermi energy simply as the excited electron. In spite of the fact the name is not strictly correct, it provides an intuitive picture that represents with good approximation what happens in metals. Note that the process of excitation will create empty states below the Fermi energy as well. Similarly to the excited electron case, this part of the exciton will be a wavepacket and will be localized in space. For shortness it will be called the hole.

In an insulator, the excited electron and the hole would create a bound state. The electron is charged negatively, while the hole positively. They will feel a strong Coulomb attraction and be bound in an hydrogen like state. To have a rough estimate of the binding energy of the electron-hole pair, we can remember that the lowest bound state of the hydrogen atom is at -13.6 eV. In a perfectly insulating material there is no way an optical laser (with photon energy around 1-3 eV) can create an electron-hole pair with energy high enough to create an unbound state.

Contrary in metals the excited electron and the hole do not form a bound state. The excited electron is not the only electron in the material feeling the positive charge of the hole. Many more electrons close to the Fermi energy are able to move and will be attracted towards the hole. They will accumulate

spatially around it and screen its electric field. The excited electron will therefore feel only a very small fraction of the attraction. No bound state will be created and the electron and the hole will be free to move independently. The effect simplistically described above is the well known dielectric screening.

In metals, also due to the dielectric screening, excited states are fairly well described by single particle wavefunctions (we have already implicitly used this approximation when we described the excitation process as the promotion of an electron from a state below the Fermi energy to above). In particular it is not a bad approximation to obtain the group velocity from the derivative of the single electron band and therefore the electron's or hole's velocity. In our case the electron will be excited from a d-level below the Fermi energy to a p-band above (see Fig 3.1.b). In transition metals the 4p band is usually very steep and electrons in it will have a high velocity, of the order of 1 nm/fs. The electron or the hole will then start travelling. In an isotropic metal the direction will be random and uniquely based on where in the Brillouin zone the excitation has happened, since the linear momentum deposited by the photon is negligible.

The electron will then travel in a straight line with a velocity that is determined by the band it is in and therefore its energy. The band and the energy define also the probability per unit time that the excited electron has to scatter. As an effect of the scattering, the electron will lose part of its energy and its momentum will be randomised. Therefore the electron coming out of the scattering will travel in a new direction on a straight line again as long as it does not experience another scattering. The complete trajectory will resemble the one in Fig. 3.1.d.

The same description applies to the diffusion of holes, with the only difference that in transition metals they are usually in less dispersive bands and therefore have lower energies compared to the excited electrons.

To give a feeling of the mobility of such electrons, the order of magnitude of the velocity of excited electrons in transition metals is around 1nm/fs. Scattering lifetimes are of the order of few tens of fs [53, 54]. This means that electrons have a mean free path of around few tens of nm. This has to be compared to the few tens of nm that are the typical thicknesses of films employed for ultrafast dynamics and, more importantly, to the penetration depth of all the optical probes. It is already evident that the effect of transport is of major importance when describing fs dynamics of nano and micro-sized materials. In the following I will show why and how in more details.

3.1.2 Scatterings and electronic thermalisation

So far we have realised that electrons and holes in metals diffuse independently after a fs excitation by a laser and that the diffusion is very fast and efficient. Nonetheless the fs exciton diffusion is strongly linked to the concept

of electronic thermalisation. To understand the interplay we have to address what happens during the scatterings in deeper details

After the excited electron experiences the first scattering the outcome is strongly dependent on the scatterer. The most relevant scattering events are either with other electrons or with phonons, defects or impurities. In the case of electron-electron scattering, the excited electron interacts with all the other electrons below the Fermi energy. The scattering cannot destroy energy, which implies that the energy lost by the excited electron is transferred to the other electrons and will create another excitation. Again in metals the outcome of an electron-electron scattering can be seen in terms of single particle excitations. An electron below the Fermi energy is ousted. It will leave a hole below the Fermi energy and create a single particle excitation above (see Fig. 3.1.c). The second excited electron will therefore start moving and will contribute to the diffusion.

This effect of creation of electron cascade is of fundamental importance because it will enhance the diffusion, through the creation of numerous carriers, but it is also the main driver of the electronic thermalisation in the system. After an electron-electron scattering the initial energy is shared between two electrons that are now closer to the Fermi energy. If the electron scatters a second time it will go to even lower energies. Eventually all the cascade electrons will tend to assume a Fermi-Dirac distribution with a very high characteristic temperature. Note that the energy provided by the photon has not exited the electronic system, the electronic population has simply rearranged itself, going from a electronic distribution very far from equilibrium to a Fermi-Dirac distribution with high temperature.

It is fundamental to include the description of the thermalisation in the model of fs transport, since 1) it happens in the same timescale as the electron diffusion, 2) the electron cascade is a fundamental part of the thermalisation process and enhances the electron diffusion and 3) when the electrons change their energy during thermalisation they dramatically change their transport properties as well. I will also show below how energy will be transported even after the thermalisation, while spin transport vanishes when the electronic system reaches a local thermal equilibrium.

Another sources of scattering are phonons, defects, or impurities. In these cases the energy is exchanged with the lattice and is removed from the electronic system. Nonetheless the amount of energy loss is much smaller than for the case of electron-electron scattering and it will lead in a longer timescale to the establishment of a common temperature between the electronic and phononic systems. The most relevant effect to the fs electron diffusion is the randomisation of the electron trajectory after each scattering.

3.2 Femtosecond exciton superdiffusion

We are now ready to tackle the problem of modelling the situation described in the previous section. We want to develop a description of the diffusion in Fig. 3.1.d, while keeping into account the fact that after every scattering the carrier can change its energy and its transport properties. Unfortunately we cannot make use of already developed transport models. As an example in Fig. 3.2, I compare different diffusion regimes of an electron travelling through a system composed of two different materials. The aim is to describe a random walk with the mean free path comparable to the dimension of the films under study (red trajectory in Fig. 3.2). It is necessary to keep track of the fact that, for instance, the electron can have a ballistic part of its trajectory that can cross two materials without scattering. Moreover it is needed to keep track of the fact that the electron can take a finite time compared to the timescale under study to cross each straight part of its trajectory.

Standard diffusion (black trajectory in Fig. 3.2) describes a random walk for the limit of mean free path and lifetime going to zero compared to, respectively, the dimension of the system and the addressed timescale. It is the limit of the process we want to describe for the number of scatterings going to infinity. On the other hand ballistic diffusion (blue trajectory in Fig. 3.2) is the limit for lifetime going to infinity, i.e. the limit for scattering probability going to zero. This limit as well is too far from the physical situation we want to describe. It is therefore necessary to describe the geometry of the diffusion for the real 3D random walk, without approximations. We also need to include in the model the energy evolution of the electrons.

I am not going to present here the complete derivation of the model, since it can be found in Papers I and II. I will, instead, just give an as intuitive as possible idea of the procedure adopted to construct the model. I will also analyse the equation and comment the physics. The most intuitive way of understanding the structure of the model is to start by splitting the complete trajectory of the electron in generations, i.e. to treat every ballistic piece of the trajectory one at a time. In this way the complete motion can be built up from the summation of the purely ballistic parts of the trajectory, by using the distribution of the end of the previous part as the starting point of the subsequent one. These parts of the trajectory will be called generations. Note that in the following I will start addressing only the kinematic problem and I will ignore for the moment the energy distribution of the electrons, which will be treated later.

It is possible to write a conservation equation for the ballistic motion of the i-th generation exciton density $n^{[i]}$ in the infinitesimal volume dV around $\mathbf{r}$ at time t as

$$\frac{\partial n^{[i]}(\mathbf{r},t)}{\partial t} = -\nabla\cdot\Phi + R(n^{[i]}) + S^{[i]} \tag{3.1}$$

where Φ is the flux vector, R is a reaction term and $S^{[i]}$ the source.

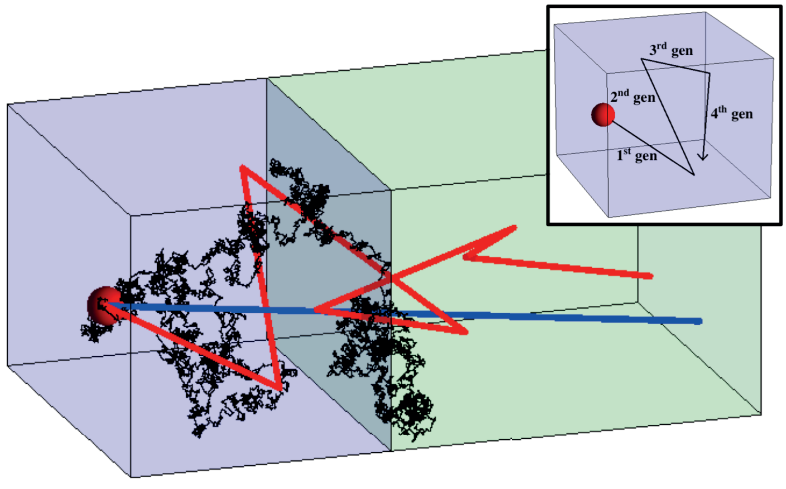

Figure 3.2. Sketch of electron trajectories for different diffusion regimes in a system composed by two different materials. In black is the trajectory of a diffusing electron in case of standard diffusion, i.e. for vanishing mean free path $\lambda \to 0$ [9]. On the opposite limit of ballistic diffusion, the blue line depicts the trajectory in the case $\lambda \to +\infty$. In our case the electron experience only a limited but non-zero amount of scatterings and travels on a trajectory that resembles the red one. Inset: Division of the motion into generations.

The flux vector keeps track of the electrons leaving the volume because they travel away from it and the ones that appear in it because of travelling in. A detailed derivation can be found for the 1D case (everything uniform along x and y) on Paper II. Even for this simpler case the functional shape is not simple and can be written as

$$\Phi^{[i]}(z,t) = \hat{\phi} S^{[i]} = \int_{-\infty}^{+\infty} dz_0 \int_{-\infty}^{t} dt_0 \, S^{[i]}(z_0,t_0) \, \phi_\delta(z,t|z_0,t_0), \tag{3.2}$$

with

$$\phi_\delta(z,t|z_0,t_0) = \frac{\widetilde{[\Delta t]}}{2(t-t_0)^2} \exp\left[-(t-t_0) \frac{\widetilde{\left[\frac{\Delta t}{\tau}\right]}}{\widetilde{[\Delta t]}} \right] \Theta[t-t_0-|\widetilde{[\Delta t]}|], \tag{3.3}$$

and

$$\widetilde{[\Delta t]}(z|z_0) = \int_{z_0}^{z} \frac{dz'}{v(z')} \quad \text{and} \quad \widetilde{\left[\frac{\Delta t}{\tau}\right]}(z|z_0) = \int_{z_0}^{z} \frac{dz'}{\tau(z')\,v(z')}, \tag{3.4}$$

and where I have defined the operator $\hat{\phi}$. In the above formulas I have used $\tau(z)$ and $v(z)$ respectively for the exciton lifetime and velocity, which can be

material- and therefore position-dependent. The expression of the flux above is dramatically different from the one in standard diffusion

$$\Phi_{st}(z,t) = -D(z)\frac{\partial n(z,t)}{\partial z}, \tag{3.5}$$

where D is the diffusion coefficient. Apart form the more complex functional dependence, the reader should note that 1) the flux in Eq. 3.5 depends on the density while the one in Eq. 3.2 depends on the external source and that 2) Eq. 3.5 is local both in time and space while Eq. 3.2 is not. In standard diffusion, electrons lose immediately the memory of the past trajectory, since the momentum is completely randomised after a scattering and the electron undergoes an infinite amount of scatterings in any unit of time. Instead for ballistic transport the electron moment remains constant and the memory is infinitely long. In the case above the memory perdures as long as the electron does not scatter, which is a finite time and not infinitesimal as in standard diffusion.

The reaction term in Eq. 3.1 describes the amount of excitons that leave the infinitesimal volume because they are scattered and, by definition, they don't belong anymore to the i-th generation, but will be the source of the (i+1)-th. Given that the probability of scattering per unit time is not affected by the past history of the exciton, the reaction gets the simple form

$$R(n^{[i]}) = -\frac{n^{[i]}(z,t)}{\tau(z)}. \tag{3.6}$$

Note that this goes beyond the relaxation time approximation in the Boltzmann equation. In the latter approximation many more simplifying assumptions are made: 1) lifetime independent on energy, 2) each scattering thermalizes immediately the excited distribution, 3) spatial inhomogeneities are dramatically approximated and energy transport cannot be modelled. The equation above states only the scattering rate, with energy dependent lifetimes. The temporal evolution of the energy of the excited particles will be fully treated below in a way that is analogous to the Boltzmann equation without the relaxation time approximation.

The source $S^{[i]}$ in the point $\mathbf{r}$ and time t is the number of excitons that enter the i-th generation at that time in that position. For the first generation the source term is simply the electrons excited by the external laser

$$S^{[i]} = S^{ext}(z,t). \tag{3.7}$$

For the subsequent generations the source is the number of (i-1)-th generation electrons that become i-th generation after a scattering. It is an excellent approximation to assume that the scattering event is very localised in space and time, therefore an (i-1)-th generation exciton being scattered at position $\mathbf{r}$ and time t will become an i-th generation one with the same coordinates.

Nonetheless it is convenient to describe a more general case in which the exciton advances generation with probability p and is destroyed with probability $1-p$. It will turn out to be useful when I will introduce the energy dependence of the exciton transport, since upon scattering the energy can be changed and one (i-1)-th generation exciton will not contribute to the i-th generation at the same energy but at a different one. We can therefore write the source term as

$$S^{[i]} = \hat{S} n^{[i-1]} = p(z) \frac{n^{[i-1]}(z,t)}{\tau(z)} \quad \text{for } i > 1, \tag{3.8}$$

where I have defined the operator $\hat{S}$.

It is now possible to construct the equation describing the density of excitons at any generation by deriving an equation for the sum $n = \sum_{i=1,\infty} n^{[i]}$. Given the linearity of the Eq. 3.1, that is an easy task and is obtained by simply summing up all Eq. 3.1 for all the generations

$$\begin{aligned} &\sum_{i=1,\infty} \frac{\partial n^{[i]}(\mathbf{r},t)}{\partial t} = \\ &-\nabla\cdot\hat{\Phi} S^{ext} - \sum_{i=2,\infty} \nabla\cdot\hat{\Phi}\hat{S} n^{[i-1]} - \sum_{i=1,\infty} \frac{n^{[i]}(z,t)}{\tau(z)} + S^{ext} + \sum_{i=2,\infty} \hat{S} n^{[i-1]} \end{aligned} \tag{3.9}$$

that in the 1D case becomes

$$\frac{\partial n}{\partial t} + \frac{n}{\tau} = \left(-\frac{\partial}{\partial z}\hat{\phi} + \hat{I} \right) \left(\hat{S} n + S^{ext} \right), \tag{3.10}$$

where $\hat{I}$ is the identity operator.

The energy dependence can be included easily by using a more complex structure for the i-th generation source term

$$\hat{S} n^{[i-1]}(E,z,t) = \int p\left(E,E',z\right) \frac{n^{[i-1]}(E',z,t)}{\tau(E',z)} dE' \quad \text{for } i > 1, \tag{3.11}$$

and having energy dependent velocities and lifetimes. The treatment above can be readily used to describe the heat diffusion. The energy associated to a particle density $n(E,z,t)$ is simply E. The energy diffusion is then given by the evolution of the energy density

$$\mathscr{E}(z,t) = \int E\, n(E,z,t)\, dE. \tag{3.12}$$

3.2.1 Diffusion regimes

From Fig. 3.2 it is evident that the diffusion modelled in the previous paragraph is a more general case of both ballistic and standard diffusion. It is

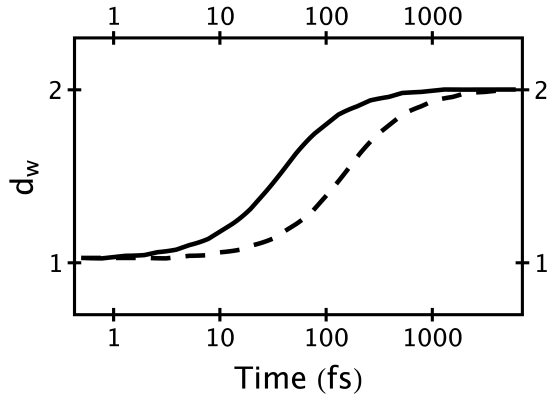

Figure 3.3. Time evolution of the anomalous diffusion coefficient d_w as defined in Eq. 3.15, numerically computed for a particle with constant velocity and an elastic lifetime $\tau = 10\,\text{fs}$ (full curve) or $\tau = 40\,\text{fs}$ (dashed curve).

possible to recover the two limit cases by taking the appropriate limits. To recover the ballistic diffusion regime one has to extract the limit for $\tau \to \infty$. The derivation of the standard diffusion is less easy but can be obtained by taking the limits $\tau \to 0$ and $v \to \infty$, with the ratio $D = v^2\tau/2$ constant and equal to the diffusion coefficient.

Nonetheless standard and ballistic diffusion are not the only two diffusion regimes used in literature. There exists a wide field on anomalous diffusions. To characterise them one usually starts from the definition of variance of the displacement σ^2 for a point source. The variance σ^2 is computed as

$$\sigma^2(t) = \int n(t,z)\,(z-z_0)^2\,dz, \tag{3.13}$$

where $n(t,z)$ is the particle distribution after time t for a Dirac δ-source in space and time. The different generalised diffusion regimes are characterised by the diffusion coefficient, which defines the exponent with which the variance of the displacement σ^2 grows with time t

$$\sigma^2 \propto t^{2/d_w} \tag{3.14}$$

where d_w is called anomalous diffusion exponent. It is easy to show that for ballistic and standard diffusion it is $d_w = 1$ and $d_w = 2$ respectively. All the diffusion regimes with $d_w > 1$ are called superdiffusive, while if $d_w < 1$ they are subdiffusive.

The case analysed in the previous section has a more complex diffusion regime. It does not have any fixed anomalous diffusion exponent, since it changes in time. A possible generalised definition of the anomalous diffusion exponent is

$$d_w(t) = \frac{2}{t}\frac{\sigma^2}{d\sigma^2/dt}. \tag{3.15}$$

In the real case of diffusing excitons the time behaviour can be rather complicated because during the thermalisation the exciton lifetimes and velocities can change. To have a qualitative understanding of what drives the time dependence of the anomalous diffusion coefficient and what are the diffusion regimes that are traversed, it is good to analyse the simple case of a particle diffusing according to Eq. 3.10 with a fixed energy, velocity and lifetime. In Fig. 3.3 the time evolution of $d_w(t)$ is shown in the two cases of lifetime $\tau = 10fs$ (full line) and $\tau = 40fs$ (broken line). The reader can observe that for times that are short compared to the lifetime the particle has a very high chance to be still in the first generation and therefore to have been travelling only on a straight trajectory. This means that the distance from the point source increases linearly with time, giving $d_w(t)$ very close to the ballistic limit. On the other limit, for timescales that are much larger than the lifetime, the particle has experienced a very high number of scatterings and therefore the diffusion is close to the limit of infinite number of scatterings. In between there is a smooth transition between the two regimes. The case of lifetime $\tau = 40fs$ is just a rescaling of the case with $\tau = 10fs$. Their behaviour coincides if the last one is dilated in time fourfold. In a logarithmic graph as in Fig. 3.3, that turns out to be a simple translation. Note that the evolution between different diffusion regimes does not depend on thermalisation but it is a characteristic of a random walk with finite mean-free-path and lifetime.

3.2.2 Transport properties of real materials

Knowledge of transport properties of real materials is of fundamental importance to predict transport effects in the femtosecond timescale. Precise calculations of these quantities are beyond the scope of this thesis and require many-body *ab initio* techniques. I will give just a short overview of transport properties of excitons in real materials. I will also propose some methods to have a intuition of the basic physical mechanism that drives the energy dependence of the transport properties. The same arguments can be used to have a qualitative prediction from the density of states of the material.

Data for velocities and electron-electron scattering lifetimes (electron-phonon and other scatterings are not included) of excited states computed with GW approach [53, 54] are shown as red dots in Fig. 3.4 for few monoatomic metals. Looking for instance at the case of Pt, one can see that group velocities of excited states can be very different from the electron velocity at the Fermi energy. This becomes obvious by considering that electrons occupy very different bands according to their energy, as can be seen from the density of states. In the case of Au excited electrons have more or less the same velocity as electrons at the Fermi energy. However if one considers the lifetimes the difference between excited states becomes very important. Before proceeding to understanding the physical implications of the transport properties of each

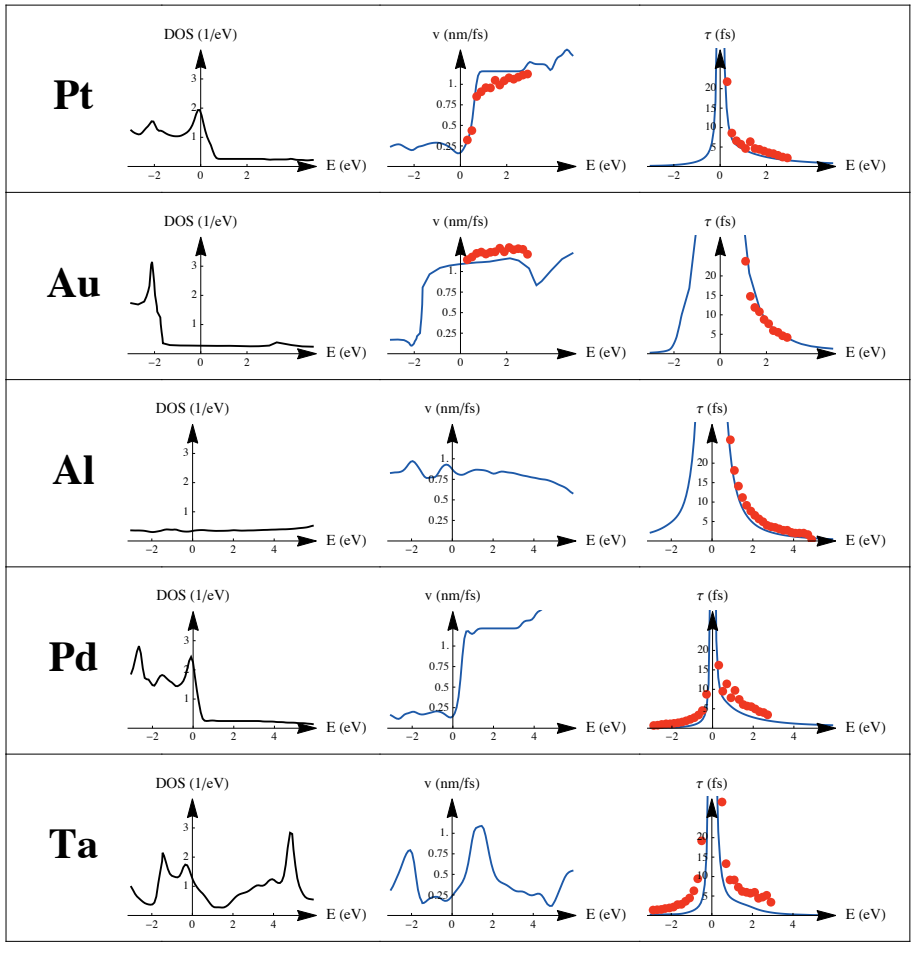

Figure 3.4. Total density of states, quasiparticle velocity and lifetime for several monoatomic metals. The density of state is computed *ab initio* [53, 54]. The red dots represent *ab initio* values for velocities and lifetimes [53, 54]. The blue lines represent the approximated velocities and lifetimes guessed with Eqs. 3.21 and 3.3.1 respectively.

single material it is useful to develop some intuition and the ability to predict at least qualitatively the behaviour of a material without employing expensive numerical methods to compute them *ab initio*.

In the case of the single particle picture the group velocity $\mathbf{v}$ of a wavepacket of Bloch levels around a wave vector $\mathbf{k}$ (in a single band) is proportional to the gradient of the energy dispersion $\mathscr{E}(\mathbf{k})$ at that wave vector $\mathbf{k}$ [1]

$$\mathbf{v}(\mathbf{k}) = \frac{1}{\hbar}\frac{\partial \mathscr{E}(\mathbf{k})}{\partial \mathbf{k}}. \tag{3.16}$$

The average amplitude of the velocity of wavepackets at an energy E is given by

$$v(E) = \frac{1}{\hbar\, S(E)} \int_{S(E)} \left| \frac{\partial \mathscr{E}(\mathbf{k})}{\partial \mathbf{k}} \right| \frac{dS}{4\pi^3}, \tag{3.17}$$

where $S(E)$ is the surface of constant energy in the reciprocal space. If we suppose that the material we are interested in is fairly isotropic we can write

$$v(E) \propto \left| \frac{\partial \mathscr{E}(\mathbf{k}(E))}{\partial \mathbf{k}} \right|. \tag{3.18}$$

The density of states $g(E)$ is instead defined as

$$g(E) = \int_{S(E)} \frac{1}{\left| \frac{\partial \mathscr{E}(\mathbf{k})}{\partial \mathbf{k}} \right|} \frac{dS}{4\pi^3}, \tag{3.19}$$

which, under the same condition, can be rewritten as

$$g(E) \approx \frac{S(E)}{\left| \frac{\partial \mathscr{E}(\mathbf{k}(E))}{\partial \mathbf{k}} \right|} \propto \frac{S(E)}{v(E)}. \tag{3.20}$$

The above equation gives an approximate relation between the density of states and the average group velocity under the assumption of single band. The area of the isoenergetic surface is unfortunately energy dependent. Even so for highly dispersive bands and supposing the band bottom at an energy sufficiently below the Fermi energy (as for instance the s or p bands above the Fermi energy in the materials showed in Fig. 3.4), $S(E)$ is approximately constant with energy and allows us to write

$$v(E) \propto \frac{1}{g(E)}. \tag{3.21}$$

This assumption becomes more shaky for more localised bands. Moreover having more bands at the same energy invalids the argument above. Finally no many-body effects are considered. In spite of that the above formula provides a very easy and intuitive way to have a qualitative idea of exciton velocities in

a real material simply by looking at its density of states. In Fig. 3.4 predictions of velocities using Eq. 3.21 are provided, where for all the materials the same proportionality constant has been used.

It is possible to have also a qualitative prediction of electron-electron scattering lifetimes. The scattering lifetime is inversely proportional to the probability of scattering. The latter is proportional to the number of possible final states. Analogously to the theory of quasiparticle lifetimes for a Fermi liquid we can give an estimation of the number of possible scatterings. The electron scattered can decay to a lower energy in a number of ways that is proportional to the integral of the density of states from the Fermi energy to its initial energy. But at the same time a second electron is ousted from below the Fermi energy and excited to an empty state above the Fermi energy. The number of ways the latter electron can be excited is again proportional to the same integral of the density of states. Therefore in a first approximation and supposing the metal has a behaviour similar to a Fermi liquid, the lifetime of an exciton can be estimated as

$$\tau(E) \propto \frac{1}{\left(\int_{E_F}^{E} g(E')\,dE'\right)^2}. \tag{3.22}$$

In Fig. 3.4 estimations of the lifetimes done using Eq. 3.22 and the same proportionality constant for all the materials are reported. One can see that most of the materials follow with acceptable approximation the Fermi liquid behaviour.

The above arguments are mainly intended to give an intuitive understanding of the physics underlying the transport properties. They will be used in the following when comparing the transport properties of spin channels in ferromagnetic materials.

On the other hand electron-defects, electron-impurity and electron-phonon scatterings have a more complex behaviour and are also strongly sample dependent. They nonetheless contribute to the total lifetime according to the rule

$$\frac{1}{\tau} = \frac{1}{\tau_{e-e}} + \frac{1}{\tau_{e-d}} + \frac{1}{\tau_{e-i}} + \frac{1}{\tau_{e-ph}}. \tag{3.23}$$

In particular these other sources of scatterings will lift the divergence of the total lifetime for energies close to the Fermi energy.

3.2.3 Thermalisation and switching off of the energy transport

It is now possible to develop some physical intuition of the processes that happen after a femtosecond laser excitation of a material. As an example I will study the excitation by an optical femtosecond pulse at the surface with vacuum of a thick layer of metallic Pt.

Right after the pulse, electrons are excited above the Fermi energy up to the energy of the photons. They will have a velocity of the order of $1\,nm/fs$,

but will have a very short electron-electron lifetime (see Fig. 3.4). They will scatter almost immediately and create a cascade of electrons, with lower energy but higher lifetime. The latter are the electrons that will drive the greatest part of the diffusion. The diffusion in this timescale will moreover be superdiffusive with a fairly high anomalous diffusion coefficient due to the long lifetimes.

The excited electron diffusion will lead to energy diffusion since the electrons will carry their energy away from the region that has been directly excited by the laser. In the meanwhile the electrons will go closer and closer to a Fermi-Dirac distribution because of electron-electron scatterings and the creation of lower energy cascade electrons. It should be noted that electrons close to the Fermi energy will have a lower velocity compared to the one excited well above (see Fig. 3.4). Nonetheless the velocity will be finite and the lifetimes, even if they will not be infinite because of other types of scatterings, will still be tens of femtoseconds. This implies that the diffusion of these electrons will be non negligible. They will therefore continue diffusing as long as the whole film will not have a spatially uniform energy distribution (with equal energy diffusing from left to right and right to left). The diffusion of thermalised electrons becomes important in bigger samples and therefore longer timescales. As shown above, the diffusion regime in longer timescales can be very well approximated by standard diffusion.

In the description above I have not mentioned the role of the holes created by the laser excitation. They will diffuse following the same mechanism as the electrons and will carry energy in the same way. In Pt holes have smaller velocities and shorter lifetimes than the electrons. Nonetheless they will contribute to the energy diffusion.

The important conclusion is that the energy diffusion continues as long as there is some spatial inhomogeneity in the electronic distribution and it is not related to the thermalisation of the electron and hole distributions, since even thermalised electrons very close to the Fermi energy will have finite velocities and lifetimes. We will see that the situation is drastically different in the case of spin transport.

3.3 Spin superdiffusion

I have show in the previous section how to describe the femtosecond diffusion of laser excited electrons and hole in metals. I have showed how simple diffusion models cannot be used. A more detailed kinematic description of the motion has had to be developed in order to bridge the short timescale, where the quasiparticle has a ballistic motion, to the long timescale, where the motion is with good approximation standard diffusive. The necessity of including a description of the thermalisation process and the physical effects of it have been finally discussed.

We are now ready to address the case of a material with two different species of carriers: a ferromagnet. In ferromagnetic transition metals the spin-orbit coupling of valence and conduction levels is very small. For this reason the spin is to an excellent degree a good quantum number. The situation is different for core levels, but these electrons are not involved in the transport described above. The electrons in the two spin channels can therefore be considered as two different species, in the sense that during the straight parts of their motion they preserve their spin character and the spin does not precess. This allows for a spin dependent description of the transport.

It is still allowed that during a scattering a carrier from one spin channel can be transformed to another quasiparticle in the other spin channel. Different scattering types lead to different spin flip mechanisms. Nonetheless all the most relevant scattering mechanisms are of electrical origin and therefore the probability of a spin flip is proportional to the spin-orbit coupling. It has always been believed that such events are rare and can affect magnetization over longer timescales. It is still under strong debate if the frequency and the efficiency of spin flip events are enhanced for femtosecond excitations in order to provide non-negligible spin flip probability before the electron system is thermalised [6, 7, 44, 21, 11, 22, 23]. Note that anyhow regardless the amplitude of the spin flip probability the arguments below hold and the possibility of spin flip can be included in the model.

It is not surprising that in a magnetic material the two spin channels can have very different transport properties. This implies that the two spin channels will diffuse in different ways. I will show below how in most ferromagnetic materials electrons in the spin majority channels have better transport properties than the electrons in the minority channel. I have shown in the previous section how each quasiparticle excitation carries its energy upon diffusing. In a similar way it carries its spin. In a typical ferromagnetic material excited by a femtosecond pulse, the consequence is that spin majority electrons will diffuse more out of the absorption region, while spin minority will diffuse much less, leading to a preferential depletion of spin up carriers in the pumped region. The reduction of the number of spin majority electrons will consequently lead to a demagnetization of that region. It has to be noted that if we assume that the probability of spin flip upon scattering is negligible, there is no absolute reduction of the magnetic moment, but simply a redistribution to regions far away from the pumped one.

3.3.1 Transport properties of ferromagnets

Again, before proceeding with the study of spin dependent diffusion, it is important to give an overview of spin dependent transport properties of a few ferromagnetic simple metals. *Ab initio* calculations show a strong spin dependence of the transport properties (see Fig. 3.5). For instance excited spin

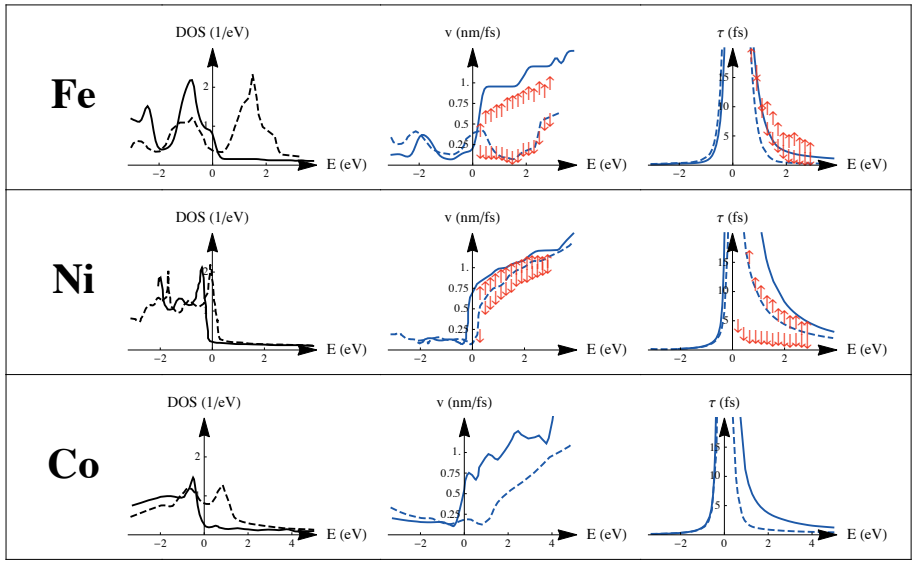

Figure 3.5. Spin dependent total density of states, quasiparticle velocity and lifetime for few monoatomic ferromagnetic metals. The density of state is computed *ab initio* [53, 54] and is displayed as a full (broken) line for majority (minority) spin channel. The red arrows up (down) represent *ab initio* values for velocities and lifetimes [53, 54] for spin majority (minority) quasiparticles. The blue full (broken) lines represent the approximated velocities and lifetimes guessed with Eqs. 3.21 and 3.3.1 respectively for the spin majority (minority) quasiparticles. The proportionality constant is the same for all the materials and equal to the one chsen for the data in Fig. 3.4.

majority electrons in Fe have higher velocities of the minority ones, while the lifetimes are not equally asymmetric. Ni instead shows a different behaviour where the strongest asymmetry is in the electron-electron lifetimes.

Using the arguments proposed in Sec. 3.2.2 it is easy to understand at least part of the origin of such strongly spin dependent behaviour. In the case of the velocity, low density of states is usually associated to highly dispersive bands and therefore to high group velocities. On the other hand, for these materials, the 3d bands have smaller dispersion and lead to high density of states but low velocities. From Fig. 3.5 one can see that the velocities predicted with the simple Eq. 3.21 have the same qualitative behaviour as the one calculated by *ab initio* methods, even though the accuracy is not satisfactory and the error not easy to predict. Note that the values have been obtained by Eq. 3.21 using the same proportionality constant as the one used to predict non-magnetic materials in Fig. 3.4, with the only difference that now the the density of states is not degenerate in spin.

A bit more attention has to be put in the qualitative extension of the reasoning proposed in Sec. 3.2.2 for the prediction of lifetimes in ferromagnetic materials. The probability of scattering is proportional to the product between

the number of available empty states for the scattered electron and the number of empty states available to the ousted electron. In principle the ousted electron does not need to have the same spin as the scattering electron. Since the aim of this analysis is to have an order of magnitude estimation, we can simply assume that the scattering can oust with equal probability an electron from the spin up or spin down channel. We can therefore guess the lifetime as

$$\tau^{\uparrow}(E) \propto \frac{2}{\left(\int_{E_F}^{E} g^{\uparrow}(E')\,dE'\right)\left(\int_{E_F}^{E} g^{\uparrow}(E')\,dE' + \int_{E_F}^{E} g^{\downarrow}(E')\,dE'\right)}. \tag{3.24}$$

The prediction, using again the same proportionality constant used for the non magnetic metals, is way less accurate (see Fig. 3.5) even though it still provides a qualitative comparison between spin majority and minority. The explanation of the deviation of the presented materials from the Fermi liquid behaviour and the failure of the simplistic description of the spin dependence of the cascade electron are beyond the aim of this thesis.

The reader has probably noted that the data presented in this section and in Sec. 3.2.2 for quasiparticle velocities and lifetimes are all theoretical ones. The reason is that experimental values have to be taken with care. The most popular technique of extraction of quasiparticle excitation lifetime above the Fermi energy is two-photon-photoemission (2PPE). A first optical laser pulse with energy lower than the workfunction of the material is shone on the sample and creates quasiparticle excitations with a distribution of energies above the Fermi level. After the excitation the quasiparticles will start decaying in energy according to their lifetime. A second optical laser pulse is then shone after a controlled delay with energy high enough to excite some of the excitons above the workfunction and lead to photoemission. The number and energy distribution of the emitted electrons is then measured over several time delays and lifetimes are extracted. The technique is usually very surface sensitive, since the quasiparticle excitations generated above the workfunction of the material have very short mean-free-paths.

This powerful technique has nonetheless a drawback in metals. What the technique measures is not the quasiparticle lifetime but an effective lifetime that is connected to the probability of finding that excited state after a certain delay close to the surface. This means that what is measured is an effective lifetime that includes scattering, transport and decays from higher energy levels. The latter is directly related to the quasiparticle lifetime and it is usually included in the analysis. Transport instead is trickier. States with long lifetimes will diffuse very efficiently away, leading to strongly reduced effective lifetimes. While states with shorter lifetimes have a smaller influence from transport. This leads to an underestimation of the lifetime asymmetry. Also injection of electrons from other layers can become extremely important in case of thin films. In the analysis of experiments the effect of transport is

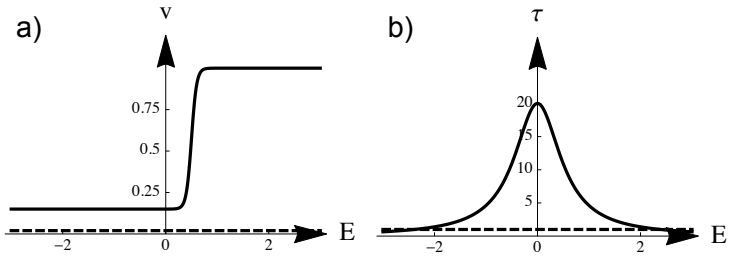

Figure 3.6. Energy and spin dependent a) velocity and b) total lifetime of electrons and holes for an ideal material with weakly dispersive bands crossing the Fermi energy for the spin majority channel; and with a spin minority channel with extremely immobile electrons and holes.

sometimes taken into account, but so far for the electron diffusion only a standard diffusion treatment has been employed. This neglects the fact that longer lifetimes lead to superdiffusive and almost ballistic diffusion of electrons out of the probed region. Using a standard diffusion description therefore leads to an underestimation of the spin asymmetry, an overestimation of the short lifetimes at high energy and an underestimation of long lifetimes at low energies.

3.3.2 Thermalisation and switching off of the spin transport

So far I have showed how electrons diffuse from the moment they are excited until the whole sample has the same energy distribution and eventually the same temperature (after all the scatterings have created a Fermi-Dirac distribution). I have also shown how spin dependent transport properties lead to spin diffusion. The careful reader can now argue that according to the above ideas, the spin diffusion should proceed as long as the whole sample has not reached a thermal equilibrium, in strong disagreement with the experiments that show that the ultrafast demagnetization switches off after some hundreds of femtoseconds.

In reality the spin diffusion does switch off when the electronic system has reached a *local* thermal equilibrium, which happens typically after several hundreds of femtoseconds. To make the explanation of the physical mechanism of the switching off more intuitive, I will describe how it works in a simplified hypothetical material and leave to the reader the generalisation to real materials. We can suppose our hypothetical material with the electrons in the spin minority channel having a vanishing velocity and a majority channel instead similar to the one of a material with a d-band crossing and below the Fermi energy and highly dispersive bands above that (see Fig. 3.6). In Fig. 3.6.a the energy and spin dependence of the velocity is shown, while the total lifetime with inclusion of electron-phonon, defect and impurity scatterings is in Fig. 3.6.b.

After the laser excitation the majority electrons will diffuse, while spin minority electrons will remain where they have been excited. This will lead to efficient spin diffusion, since the minority channel will not reduce the effect by diffusing minority spin. However electrons are not the only quasiparticle diffusing: holes diffuse as well. Above I almost always focused on the electrons only because, in most of the materials, holes have worse transport properties and contribute less to the diffusion. On the other hand when the system approaches thermal equilibrium, hole transport cannot be neglected anymore.

As we have seen in Sec. 3.2.3 the holes carry energy and they contribute strongly to the heat transport when the system reaches a local temperature. The same happens for the spin transport, with a very important difference: electrons and holes within the same spin channel carry opposite spin. This means that the energy diffusion led by holes will add up to the one led by electrons, while the spin diffusion driven by the holes has to be subtracted from the one driven by the electrons within the same spin channel.

We now consider again our ideal material. Right after the femtosecond laser excites the electronic system, electrons will be excited up to high energies and will have an high velocity. Holes will be created down to the same negative energy, but the velocity will be low. The net diffusion will be the difference between the two. After the system has reached an electronic thermalisation, all the electrons and holes will be close to the Fermi energy. Now they will have the same velocity and lifetime. They will still diffuse and carry energy, but their diffusion will be the same and the net spin transport will vanish.

3.3.3 Chargeless spin transport and dielectric screening

I have showed how electrons upon diffusion carry their energy and their spin. However electrons carry another quantity: charge. This would imply that along energy and spin diffusion, after a femtosecond laser excitation we should expect charge diffusion with the formation of regions with strong charge accumulation. In reality this does not happen because metals present a very efficient dielectric screening.

In the intuitive picture described above, after the absorption of a photon the electron-hole pair is formed. The electron and the hole can move apart. This would leave a strongly positively charged area where the hole is, and negatively where the electron is. Nonetheless all the other electrons around the Fermi energy will feel the electric field generated and will flow towards the hole or be repelled by the excited electron. The effect will be a sort of local high tide of the Fermi sea around the hole and a local low tide around the electron.

But when the excited electron or the hole moves apart they will move with their own "tidal waves". In the ideal case of perfect dielectric screening the charge of the excited electron or the hole will be completely compensated by

the decrease or increase of the electronic density around the Fermi energy. The couple created by the excited electron and the depletion of electron density at the Fermi energy will therefore be chargeless. When in the previous sections I have been referring to excited electron, what had to be read was the electron-screening electrons pair outlined above.

Note that in real metals the dielectric screening is not perfect, but the estimation of the fraction of charge that is transported by the quasiparticle excitation is beyond the aim of the present study. Finally it can be mentioned that in a magnetic material the screening can be spin polarised. This can influence the spin that is actually transported by the quasiparticle excitations. Such a treatment too is beyond the scope of the present study.

3.3.4 Energy efficiency of spin superdiffusion

The argument that scientists working within the field of spintronics use to support their research is that the use of the spin degree of freedom as a carrier of information could help increase the energy efficiency of the devices. The transport of magnetization can in principle be disconnected from the transport of charge and avoid in this way the problem of Joule heating. Yet the magnetization transport still needs to be triggered by some external stimulus, which might not be as energy efficient as hoped. For instance domain walls can be moved by the injection of spin polarised currents. Unfortunately the required currents are still high.

Superdiffusive spin transport instead is an highly energy efficient process. First, there is a very high photon-to-spin quanta conversion rate. Each photon excites directly one electron, but through the process of generation of cascade electrons many more are excited and made available for transporting information. If the electron excited is a majority spin it will diffuse away and transport spin. If it is a minority spin to be excited, the energy that it has gained is not wasted: the electron will remain where it has been excited and trigger further cascade eventually giving part of its energy to other majority electrons that will drive spin transport. For the reasons above the number of electrons actually carrying spin information generated by a single photon is much higher than 1. The actual number depends on the energy of the photon, the transport properties of the material (especially on how inefficient the transport of spin minority is and the energy range that contributes most to the spin transport) and on the geometry.

The second reason why superdiffusive spin transport is highly energy efficient is due to the almost ballistic regime of the transport. Standard charge currents rely on the small deviation of the electron trajectories due to the external field. Nonetheless the greatest part of the kinetic energy of the electron is spent in travelling towards randomly oriented directions, with zero net transport. Only the small coherent part induced by the external field can be used.

Even in the case one would be able to exploit the diffusive part of the kinetic energy, the standard diffusion regime makes this kind of transport highly inefficient. Instead, due to the almost ballistic diffusion regime of superdiffusive electrons, it is possible to make use of the whole kinetic energy of the electrons. After an excitation the front of the diffusing spin will travel at the real speed of the electrons of around 1nm/fs, a velocity of propagation of information that is unthinkable of using ohmic currents.

The drawback is that controlling superdiffusive spin transport has to be done in a passive way. Since external fields will have negligible influence on the current itself, they have to be used to modify the transport properties of the materials in the device and only through that affect the spin transport.

3.4 Extensions of the superdiffusion model and other effects

3.4.1 Saturation effects

The treatment developed so far is based on the assumption that the process modifies negligibly the material. Non-linear behaviours and saturation effects can arise from several different sources.

High intensities of the incident pump pulse can lead to non-linear effects beyond absorption or lead the material to non-linear optical responses. The absorption efficiency can also be reduced due to state-blocking. All these effects modify the initial excitation of the system under study and can be described by already developed models. For this reason I will skip them and refer the reader to the literature [30].

What is instead more relevant for the treatment is the fact that when spin is transported, the magnetization of the materials of the sample is affected as well. From an electronic point of view the populations of the two spin channels are therefore altered. It is hence not surprising that the spin dependent transport properties can be altered.

If a region of a ferromagnetic material undergoes demagnetization, it is expected that the spin asymmetry of the transport properties should diminish. The way this reduction happens is instead a way less trivial problem. It depends strongly on the electronic configuration of the material when it is demagnetised. Several different scenarios can be proposed. The topic is currently under study. For this reason I will avoid addressing the problem. In the following I am interested only in showing how transport properties are influenced by the non-equilibrium configuration of the material. As an example I will provide a way to qualitatively predict them for the most straightforward electronic configuration one can think of. Such electronic configuration does not seem to be the one assumed by the material and it will be used only as a simple example to apply the methodology.

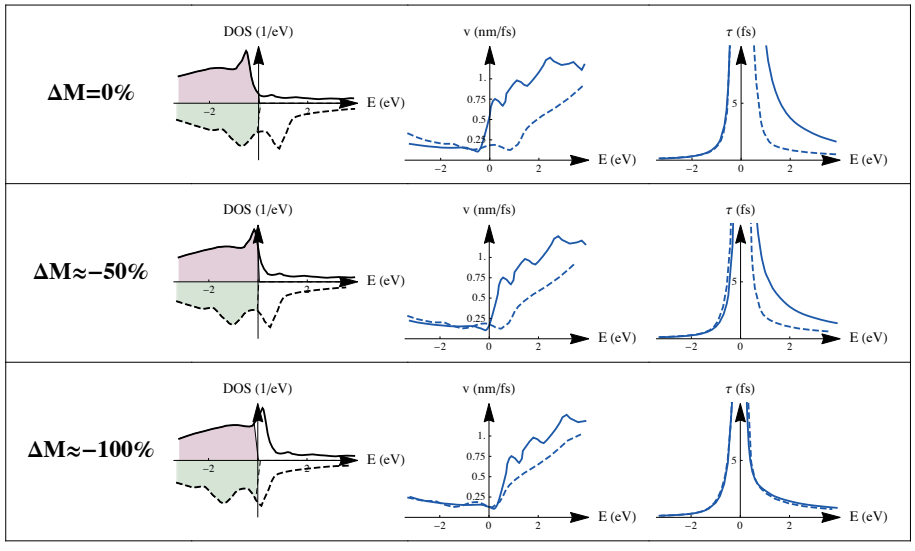

Figure 3.7. Spin dependent total densities of states (with highlighted occupation), quasiparticle velocities and lifetimes estimation for the "rigid band shift" scenario of demagnetised material.

Let us suppose that the demagnetization leads to an increase of the population of the spin minority channel, that leads to a rigid shift down in energy of the minority spin channel band structure, while similarly the majority shifts up in energy by an amount that would keep the total electron number unchanged. We can call such a scenario "rigid band shift". The density of states at different demagnetization and the populations for Co will appear as in Fig. 3.7. We can now again apply the same arguments as in Sec. 3.3.1 and estimate velocities and lifetimes (see again Fig. 3.7).

We can notice how the asymmetry of velocities and lifetimes will be reduced. In the case of velocities some difference remains even at complete demagnetization because it has been assumed that the bands are simply shifted and the repopulation does not change the shape of the density of states which might be true for small demagnetization, but is clearly expected to fail in case of big ones.

In spite of the fact that the trend above has been extracted for the very simplistic "rigid band shift" scenario of the demagnetised electronic configuration, the idea that demagnetization leads to a decrease of the spin asymmetry of transport properties is general. The effect on the spin transport is to create saturation at high laser excitations. After an intense pump from a laser pulse, the ferromagnetic material will start creating a strongly spin polarised current. As the spin diffuses the material demagnetises, the transport properties change and the outgoing current will be less and less spin polarised.

One important consequence is that a ferromagnetic material cannot be completely demagnetised by the simple ejection of spin polarised current created by a direct laser excitation. Also note that saturation effect are local. This means that regions that have been strongly demagnetised are lees likely to demagnetise more. This leads to smoother magnetization changes profiles than what one may predict by using the properties of the unperturbed material.

The model developed in Papers I and II needs therefore to be complemented with electron density dependent velocities $v\left(E,\sigma,z,t,n^{\uparrow},n^{\downarrow}\right)$ and lifetimes $\tau\left(E,\sigma,z,t,n^{\uparrow},n^{\downarrow}\right)$. As discussed above the dependence of v and τ on $n^{\uparrow}$ and $n^{\downarrow}$ is the subject of current research.

3.4.2 Drift and external fields

The effect of external fields on superdiffusing electrons has been neglected. An external field will apply acceleration to the traveling electron (or hole) and will bend the trajectory. Usually such corrections to the electron trajectory are small even for big external fields. They become important in the transport of thermalised electrons because in that case the diffusive part of the trajectories of all the electrons tend to cancel statistically and only the bends induced on the trajectories by the external field will sum up to a non vanishing value. In the case of femtosecond transport the cancellation of the diffusive part of the trajectory does not happen and their contribution can, to an excellent approximation, be neglected.

Even if the model of superdiffusive transport has been developed to describe the transport in the sub-picosecond timescale, it still describes the diffusive part of the transport in longer timescales. It can in principle be used to describe the nanosecond heat diffusion. However for such long timescales compared to the lifetime *and* for distances much longer than the mean free path, the diffusion is to an excellent approximation standard diffusive (standard diffusion is simply a limit of the superdiffusion for $t \to \infty$) and there is no reason to use the much more computationally demanding superdiffusive description.

Nonetheless even in longer timescales, if the dimensions of the system are comparable with the mean free path and the excitation has also a strong spatial confinement, the diffusion still retains the superdiffusive character. Such situation would be challenging to model since along with the anomalous diffusion regime of the diffusive part of the trajectory, the drift term because of the presence of external fields needs to be taken into account.

4. Experimental evidences of superdiffusive spin transport

In the past chapter I have described the model of superdiffusive spin transport, I have showed how spin can be transported superdiffusively and given a survey of the main physical implications of the process. In this chapter I will show how the model proposed above compares with experimental results.

In Papers I and II it has been proposed that the spin superdiffusion induces a big demagnetization after a femtosecond excitation and how it can in principle account for the total demagnetization. At that time the prediction was done completely theoretically and an already existing experiment has been modelled. Since then more and more experimental results are strongly supporting the role of superdiffusive spin transport. But the most amazing results have been showing how the use of spin currents can lead to unexpected new phenomena.

For instance in Paper III we have showed for the first time ever the effect of ultrafast increase of magnetization. This has been achieved by driving the spin ejected by a Ni layer into an Fe layer. In Paper IV we have shown how ultrafast demagnetization can be induced by excited electrons created in a neighbouring layer and not only by direct laser excitation. Finally in Paper V we made use of the very high intensity of superdiffusive spin currents to produce a THz emission via the inverse spin Hall effect. We have also showed how it is possible to tailor the spectrum of the emitted electromagnetic waves by varying the transport properties of the layers of the device,.

Together with our results, more and more experimental data from independent groups are showing the signature of spin transport. In the end of the chapter I will give a small survey of these works.

It is still unclear whether superdiffusive spin transport is the only mechanism of the ultrafast demagnetization or another mechanism contributes as well. Nonetheless, regardless of the answer to that question, the discovery of such strong spin transport in the sub-picosecond timescale is of huge fundamental and technological importance.

4.1 Ultrafast increase of magnetization

One of the most spectacular results in the field of ultrafast magnetization dynamics in the past years has been the experimental verification of the predicted

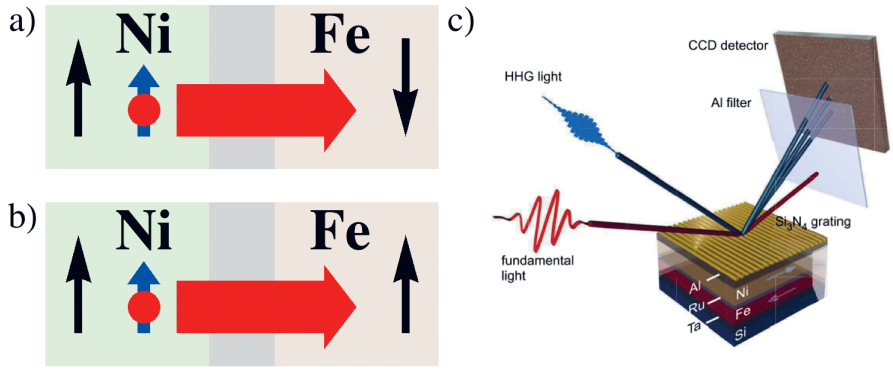

Figure 4.1. Schematic representation of the layered system used to show the ultrafast increase of magnetization. The black arrows represent the magnetization orientations of the different layers in the a) antiferromagnetic and the b) ferromagnetic configuration. In c) the schematic setup of the experiment is shown as in Paper III. The pump laser (indicated as fundamental light) is in red. The probe pulse obtained by high harmonic generation (HHG) is reflected at the surface of the sample and diffracted by a Si_3N_4 grating deposited on top of the sample in order to measure the reflection at different probing frequencies. The sample is deposited on a Si substrate.

possibility of increasing the magnetization (Paper III). For more than fifteen years the scientific community has addressed the problem of the description of the ultrafast demagnetization of ferromagnets. Several models have been proposed and several driving mechanisms put forwards, but none has ever considered the possibility of an ultrafast increase. Moreover none of the other approaches had ever addressed the possibility of the non-locality of the driving mechanism.

In Paper I the possibility of injecting magnetization in a non-magnetic material was predicted. Melnikov et al. [32] provided the experimental verification of transient magnetization induced in the non-magnetic substrate. In Paper III we have showed how it is possible to manipulate the magnetization of a ferromagnetic layer in unprecedented ways by both reducing and increasing its magnetization, depending on the relative orientation to another layer used as a reservoir of spin.

The structure of the experiment is schematically depicted in Figs. 4.1.a and 4.1.b. The two ferromagnetic layers (in our case Ni and Fe) can be coupled through a non-magnetic spacer. Depending on the thickness of the spacer, the RKKY coupling between the two can be either ferro- or antiferromagnetic. In case of antiferromagnetic coupling, in absence of or for a small external magnetic field, the magnetization in the two layers will be pointing towards opposite directions. If instead a sufficiently high external magnetic field is applied, then the two layers can be forced to align their magnetization parallel. In such a way it is possible to control within the same sample the relative magnetization orientation.

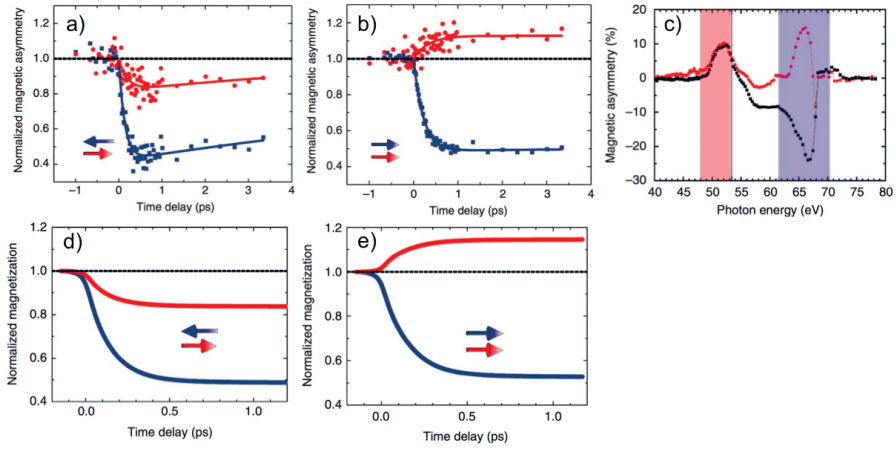

Figure 4.2. Experimental and theoretical results for the time dependence of the layer-resolved magnetic moment. In a) the value of the experimental magnetic asymmetry from Ni (blue line) and Fe (red line) for antiparallel alignment of the magnetic moments. In b) are the same values for the case of parallel alignment. The experimental magnetic asymmetries are obtained as the area of the respective edges in the time resolved spectra: in panel c) the Fe edge is highlighted in red and the Ni one in blue. In the two bottom panels the theoretical time dependence of the average magnetization in the Ni and Fe layers are shown for the c) antiparallel and d) parallel cases.

A femtosecond laser pulse can be therefore shone on the structure in the two magnetic configurations and, using the technique developed in Ref. [27], the magnetization dynamics in the two layers can be probed independently (see Fig. 4.1.c). When the film in the antiparallel configuration was irradiated, nothing unexpected happened. Both layers showed ultrafast demagnetization (see Fig. 4.2.a). On the other hand, when the experiment was performed on the system with parallel alignment the remarkable effect of ultrafast increase of magnetization was observed in the Fe layer (see Fig. 4.2.b).

An intuitive picture of the dynamics is that the laser excitation creates a flux of spin polarised electrons from Ni to Fe in both configurations. In case of antiparallel alignment (see Fig. 4.1.a), the spin up electrons removed from the Ni layer lead to a reduction of the magnetization in this layer. When they arrive in the Fe layer, they are minority and reduce the magnetization of the Fe layer as well. A similar scenario is present in the antiparallel situation as well. The fundamental difference is that the spin up electrons escaping from the Ni layer are now majority electrons in Fe as well. Trapped in the Fe layer they lead to an ultrafast increase of the magnetization. Theoretical data predict the spin accumulation in Fe and agree very well with the experimental results.

4.1.1 Reason of the directionality to the spin flux

The spin superdiffusion, being a diffusive process, cannot be directed actively i.e. by an external field. The directionality is instead caused by geometrical properties or by differences in the transport properties of the materials.

For instance the presence of the surface with the vacuum sets a preferential direction of the spin flux since optically excited electrons cannot overcome the workfunction of the material and ejected into the vacuum. Therefore those electrons that diffuse towards the surface with the vacuum are reflected back towards the substrate.

In the case of the trilayer in Paper III, the interface with the vacuum contributes to the creation of a preferential direction of the spin flux. Nonetheless the direction of the net flux is an interplay of different factors: vacuum interface, position of other layers and transport properties of the different materials. It has to be noted that for instance the transport properties of the Fe are in general worse for both spin channels than the Ni (see Fig. 3.5). This follows from the fact that the most effective transport is done in the energy region around 0.5 eV (because of the high number of excited electrons in this energy range and because of the high lifetimes). But at these energies the electron-electron lifetimes tend to diverge. The consequence is that the total lifetime will be set mainly by electron-phonon, electron-impurity, electron-defect scatterings which are not strongly energy and spin dependent. Therefore a general idea of the transport can be developed by looking at the quasiparticle velocities in this range. The Fe has in this energy range overall lower velocities than Ni.

Another effect that comes into play is the probability of trapping electrons with a given spin in a layer. If the material has to increase its magnetization because of spin injection, the incoming spin majority electrons have to occupy empty spin majority states. In Fig. 3.5 the reader can compare the density of states for Ni and Fe. While Fe has some empty d states in the majority band and can host electrons there, the majority spin d band in Ni is completely below the Fermi energy. For this reason it is less likely that an incoming spin majority electron will be trapped in Ni rather than in Fe.

4.1.2 Saturation and competing effects

The effect of ultrafast increase of magnetization in the trilayer in Paper III, has been observed for a range of fluences. However for high fluences the Fe layer demagnetises even in the parallel alignment case.

The reason for such behaviour is not clear. In Sec. 3.4.1 I have shortly discussed the importance of studying saturation effects. These are not included in the theoretical description used in Paper III. Unfortunately the effect of non linear effects is hardly predictable in the used sample because of the presence of several layers (in Fig. 4.1 a very simplified sample structure has been presented, while the real one is Al(3nm)/Ni(5nm)/Ru(1.5nm)/Fe(4nm)/

Ta(3nm)/Si(substrate)). For instance different materials can show non-linear behaviours at different fluences. Even more difficult to predict intuitively is a situation where, for instance, an initial saturation of al layer can lead to a increased flux penetrating the next one. Such energy injection can then trigger an enhanced spin diffusion from the second layer, drastically changing the sing on the overall diffusion.

Another highly probable explanation is that another process, that always drives local demagnetization, coexists with spin superdiffusion after the laser excitation. At low and medium fluences the spin superdiffusion prevails and dictates the magnetic behaviour of the system, while at high fluences the transport mechanism saturates and the local mechanism wins leading to a decrease of the magnetization.

The experiment in Paper III does not allow distinguishing between the two mechanisms above and moreover, before the development and verification of a model for non linear effects, it in not clear if the full treatment of spin superdiffusion can model such a behaviour. The question about the driving mechanism of the behaviour at high fluences remains still open.

4.2 Ultrafast demagnetization driven by excited electrons

In Paper IV we have shown that direct light irradiation is not a prerequisite for the ultrafast demagnetization. Differently from Paper III, where part of the demagnetization in Fe was driven by the direct injection of spin polarised electrons, here we show how spin unpolarised electrons diffusing from a non magnetic layer into the magnetic one trigger the demagnetization, by releasing their energy in the magnetic layer. The immediate consequence is that the ultrafast demagnetization does not rely on the photon itself, but simply requires the energy.

To achieve the result the demagnetization of a typical sample for ultrafast demagnetization experiments Ni/Al (more specifically Pt(2.5nm) / Ni(20nm) / Pt(2.5nm) / Al(substrate) as in Fig. 4.3.a) has been compared to the demagnetization of a similar sample Au/Ni/Al where the ferromagnetic layer has been covered by 30nm of Au (Au(30nm) / Ni(15nm) / Pt(2.5nm) / Al(substrate) as in Fig. 4.3.b).

The demagnetization dynamics of the ferromagnetic layer have been probed by XMCD. The experiments show a standard demagnetization curve in the case of the Ni reference layer (blue line in Fig. 4.3.c). However the demagnetization in the Au capped case shows a longer decay time, but more importantly a delay (red line in Fig. 4.3.c).

We explained this by superdiffusive transport of electrons. The laser pulse excites electrons in the Au layer. Such electrons are not spin polarised and in Au will have long lifetimes. Upon reaching the Ni layer spin majority

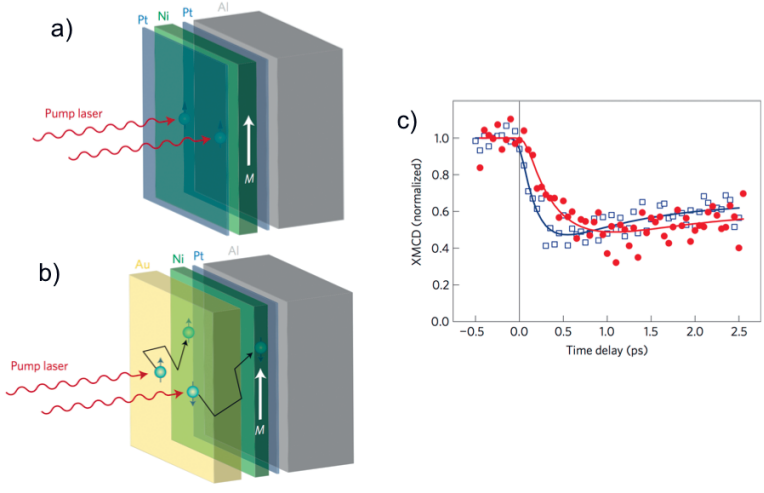

Figure 4.3. Structure of the samples and time resolved XMCD signals (figures from Paper IV). In panel a) the structure of the Ni/Al sample is shown, together with the pumping laser. The electrons that trigger the ultrafast demagnetization are immediately excited by the laser. In panel b) the Au/Ni/Al sample is shown. The electrons in the Ni layer triggering the ultrafast demagnetization are now excited by the scattering of the spin unpolarised electrons excited by the laser in the Au layer and then diffusing towards the Ni layer. In Panel c) the time resolved XMCD signal is showed for the Ni/Al reference (blue) and the Au/Ni/Al (red).

electrons will still have good transport properties and will eventually escape into the other layers. Instead the spin minority will suddenly experience a worsening of the transport properties. They will therefore get stuck in the Ni layer and deposit their energy there. By the process of electron cascade they will trigger electronic excitation very similar to direct light absorption. This will lead to the demagnetization of Ni.

The effect described above requires the electrons generated in the Au layer to reach the Ni. At a finite speed, this will take a finite time. At the same time the direct laser excitation of the Ni will trigger the standard demagnetization. In the case the demagnetization coming from the direct excitation of Ni is smaller than the demagnetization induced by the excited electrons diffusing from the Au layer, a delay in the drop in the magnetization is expected. This explains the delay in the magnetization drop in the Au capped case.

4.2.1 Incorrect absorption profile

In the original article we have estimated the layer resolved absorbed power using the Beer-Lambert law and the dielectric response of perfectly crystalline Au and Ni. The calculated absorption profile was then used as input for the superdiffusive spin transport calculations. Such scenario predicted that, in the

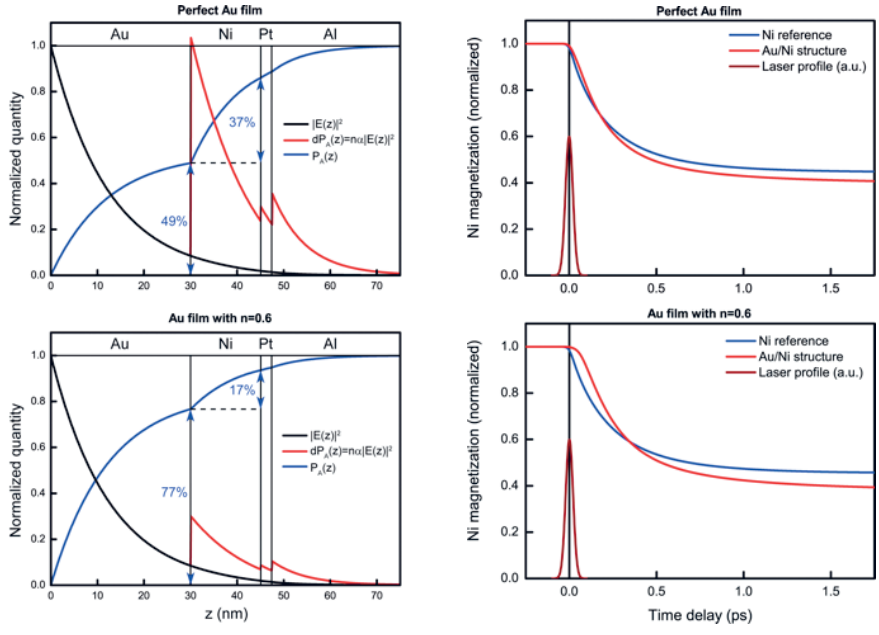

Figure 4.4. The absorption profile of the light in the Au capped sample is shown on the left in the two cases of perfectly crystalline Au (top) and imperfect Au (bottom). The square of the electric field (shown in black) is not directly representative of the deposited power, that is instead drawn in red. The total power deposited by light up to depth z is shown in blue. On the right there is the time dependence of magnetization of the Ni layer in red for the Au capped structure and in blue for the Ni reference sample. Again, the top panel shows the case of perfectly crystalline Au, while the bottom panel shows the case of imperfect Au.

Au capped case, 90% of the non-reflected power was absorbed into the Au layer and only 7% in the Ni.

It was brought to our attention [19, 38] that the formula we have used was incorrect and that the absorbed power is instead proportional to the electric field amplitude squared multiplied by the real part of the refractive index and not to the square of the electric field only:

$$P(z) \propto n(z)\,|E(z)|^2 . \tag{4.1}$$

Using the dielectric properties of perfectly crystalline Au and the correct formula for the absorbed power, the absorption scenario is different from what we estimated at first. Of the light penetrating the surface, 49% is absorbed into the Au and 37% is instead absorbed in the Ni layer (see top-left panel in Fig. 4.4). A strong direct excitation of the Ni layer is predicted differently from what we had assumed in Paper IV. Such absorption scenario weakens the conclusions drawn in the paper, since now a qualitative difference is not expected anymore, but only a quantitative difference. Nonetheless the absorption profile predicted with the correct formula leads to some incongruences

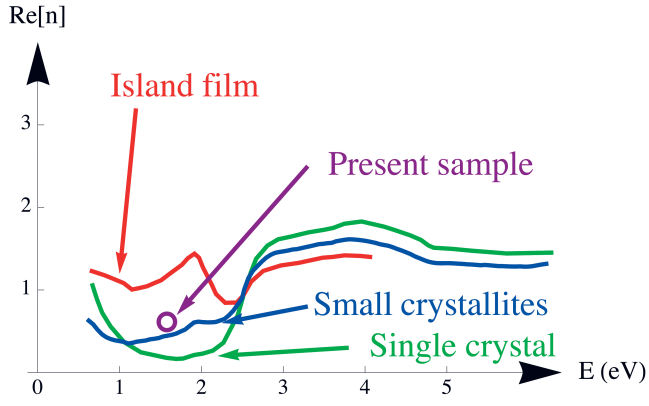

Figure 4.5. Changes in the real part of the refractive index due to reduced degree of crystallinity in Au, going from "Single crystal", through "Small crystallites" to "Island film" . The curves are taken from [46]. The purple circle highlights the value of the real part of the refractive index for Au in the Au/Ni/Al sample, extracted from the reflectivity.

with the experimental results that can be solved by recalling that structural defects in Au lead to strong variation of the refractive index in the optical range, as will be shown below. In spite of the fact that the explanation below gives a consistent explanation and seems to agree well with both past and ours experimental results, further experiments are definitely needed to clarify whether the conclusions are correct.

Using the refractive index for perfect single crystal Au, the estimation of the reflectivity at the interface with the vacuum is 95%, while the measured one is 88%. As showed in Ref. [19], such kind of calculations (Maxwell's equations for the multilayer structure) predicts excellently well the experimental values. Therefore such strong discrepancy cannot be ascribed to imprecisions of the theory. Moreover if we compute the demagnetization due to superdiffusive spin transport (see top-right panel in Fig. 4.4), no delay is predicted, contrarily to experiments that show a clear delay. The reader should note that assuming that another driver of ultrafast demagnetization is active will predict again no delay and and provide a scenario even more in contrast with the experimental results.

If one then assumes that the Au in the sample is simply not perfectly crystalline (which is common for sputtered films) all incongruences are lifted. Théye [46] showed how non perfectly crystalline Au has a strongly modified refractive index in the energy range 1-2 eV (see Fig. 4.5). Specifically increasing degree of non-crystallinity leads to a strong increase of the refractive index and therefore to a reduction of the reflectivity. We extracted from the measured reflectivity the refractive index of the Au layer. This leads to n=0.60 (shown in purple in Fig. 4.5) while k retains approximately the value

of perfect Au (as showed in Ref. [46]). Calculating the absorption scenario in this case leads to 77% of absorption in Au and 17% in Ni (see bottom-left panel in Fig. 4.4). Calculations of spin superdiffusion lead to good agreement with the experiments and show that the delay in the demagnetization for the Au capped case is present (see bottom-right panel in Fig. 4.4).

4.2.2 Spin transport to distant layers

Regardless of the correctness of the absorption profile, the experimental results show a clear delay of the demagnetization for the Au capped sample, while in the Ni reference the demagnetization starts immediately. For a quantitative analysis a precise absorption scenario is needed, but qualitative conclusions can be drawn even if the correct one is not known.

The delay shows that ultrafast demagnetization triggered by electrons traveling from the Au layer is much bigger than the one driven by spin superdiffusion of the electrons excited by the laser immediately in the Ni layer. It is moreover bigger than any other mechanism that would drive demagnetization in the Ni after the laser excitation.

We have thus shown how the ultrafast demagnetization does not need a direct laser excitation and therefore the presence of the electric field, but requires only excited electrons. Strictly speaking a mechanism that would require only the energy but not the electric field could still play a role and cannot be excluded with this experiment. Nonetheless the discovery of laser-free ultrafast magnetization dynamics is of huge fundamental importance, since it shows that the spin information transported by spin bunches can be directly used in other parts of the device to write distant magnetic layers.

4.3 Generation of tuneable THz radiation by spin currents and inverse spin Hall effect

After having proved the existence of superdiffusive spin currents, we have used them to produce a first device in Paper V. As already pointed out above, the direction and the temporal profile of the spin current are strongly affected by the geometry of the sample and the transport properties of the materials. We have therefore used this idea to design spin currents with very different temporal profile. Two samples have been prepared where a ferromagnetic layer (10 nm of Fe) has been capped with 2 nm of two different materials with strongly different transport properties: Ru, with small velocities and short lifetimes and Au where instead the p states have high quasiparticle velocities and lifetimes. The predicted spin currents in the two samples are very different as shown in Fig. 4.6.

Measuring a spin current directly is far from trivial. Typical magneto-optical techniques do not provide a direct access to spin currents. They mea-

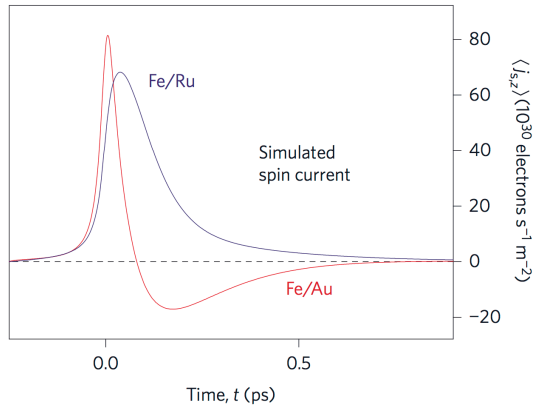

Figure 4.6. Theoretically predicted spin currents at the layers interface in the Fe(10 nm)/Au(2 nm) and Fe(10 nm)/Ru(2 nm) Fe(10 nm)/Au(2 nm) samples, in red and blue respectively. It can be seen that in the case of the Ru capped sample the spin flux is always from the Fe layer towards the Ru. Instead in the case of the Au capped sample the flux is towards the Au at the beginning but then the sign of the current changes and there is a partial backflux of the spin that has been injected in the Au.

sure only the magnetization dynamics and not the spin current itself. In principle one could extract the current from the time dependence of the magnetic signal, but this requires the assumption that the magnetization dynamics come only from spin transport. This is still to be proven. Moreover optical techniques would provide some linear combination of the time-dependence of the magnetizations in the two different layers.

We therefore need a method that would allow us to address the spin current directly. But this is a very challenging task. Spin currents are already more elusive than charge currents. Moreover standard electronics poses tough difficulties if one tries to use it at such high frequencies as in the THz regime. Finally adding contacts to the sample increases dramatically the complication of the sample preparation and lead to a far more complicated transport scenario.

The approach used is based on a direct contact-less detection of the spin current and can be divided into 3 steps:

- *conversion of spin current into a charge current via inverse spin Hall effect*
  The technique has been recently used successfully to convert spin currents into charge currents in the static case [37]. Due to spin-orbit interaction an electron with a definite spin, travelling in a direction orthogonal to its spin, is subject to a transversal deviation of its trajectory. An electron with opposite spin travelling in the same direction instead has its trajectory deflected in the opposite way. In case we have a non spin polarised current, we will observe spin separation. This effect is known

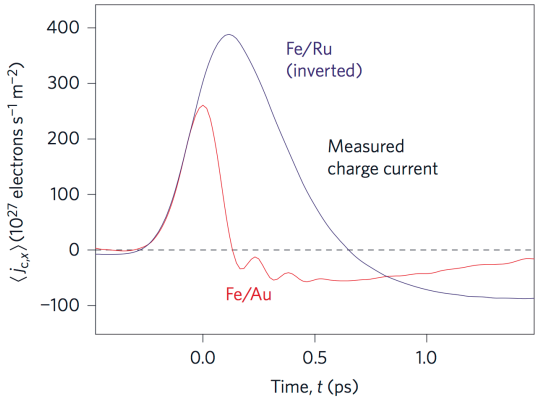

Figure 4.7. Measured transversal charge currents in the Fe(10 nm)/Au(2 nm) and Fe(10 nm)/Ru(2 nm) Fe(10 nm)/Au(2 nm) samples, in red and blue respectively.

as spin Hall effect. Instead, in case of a pure spin current, a net transverse charge current (orthogonal to the current direction and the magnetic moment) can be measured due to the asymmetry in the number of deflected electrons leading to the inverse spin Hall effect (ISHe).

- *emission of electromagnetic radiation by the generated charge current*
  The charge current generated in the previous step runs across the surface of the sample and creates an efficient geometry for emission of electromagnetic radiation. In spite of the fact that the ISHe coefficient is small the predicted spin currents are extremely high. Therefore the charge current generated is expected to have sufficient amplitude to produce a detectable THz signal outside the sample.
- *detection of THz signal and inversion of Maxwell's equation to obtain the generating current*
  The detected signal is the effect of the temporal shape of the current generating it, the propagation outside the sample and the detector's response. By knowing the detector's response function, the attenuation and distortion during propagation, the temporal shape of the current generating it can be obtained.

The measured currents agree well with the predicted ones (see Fig. 4.7). Note anyhow that the currents shown in Fig. 4.7 are the charge currents. The experimental spin current has to be extracted by dividing by the ISHe coefficient. The order of magnitude and the sign have been estimated by computing the spin Hall coefficient (see Supplementary information in Paper V).

The most important conclusions that can be extracted are four. 1) The inverse spin Hall effect still works at high frequencies and can be used to convert spin currents into electrical currents. This is, so far, the only way to measure directly THz spin currents. Moreover detecting the THz field emitted is a non-invasive and contact-less way to address the spin currents. 2) We have

showed that the temporal shape of spin currents can be designed by accurate use of multilayers with materials with appropriate transport characteristics. This is the basis of a first spin-electronic device: a pulse shaper. 3) The Fe/Au structure has a very broad spectrum of THz emission, reaching the record bandwidth between 0.3 to 20 THz and covering the range between 5 and 8 THz, where semiconducting emitters suffer of emission gap due to phonon resonances. 4) We have unveiled the microscopic origin of the THz emission associated to the ultrafast demagnetization.

4.4 Further experimental confirmations of superdiffusive spin transport

First evidence of spin transfer

The first evidence of the role of transport in the ultrafast demagnetization was actually provided by Malinowski *et al.* in Ref. [29] before I proposed the model of superdiffusive spin transport. They compared the demagnetization time and amplitude of multilayer stacks of Co-Pt for different relative orientation of successive layers and different kinds of interlayers. They reported a higher demagnetization in case the ferromagnetic layers were oriented in an antiparallel way with respect to the parallel alignment. They interpreted the difference as a sign of spin transfer between the two layers, and the demagnetization in the case of parallel alignment as driven by a local process. In principle the results from Ref. [29] can be explained completely by spin diffusion. The authors underestimated the spatial extent of spin diffusion, and the decrease of the optical signal measured at the outermost layers is partially due to spin superdiffusion to deeper layers. It is instead not possible to exclude the presence of other mechanisms.

Magnetisation transfer to non-magnetic metal

After I proposed the model of spin superdiffusion further experimental evidence was reported by Melnikov *et al.* in Ref. [32]. In the experiment an Fe/Au sample is pumped by an optical femtosecond pulse from the ferromagnet side, while the magnetic signal is measured by second harmonic generation from the Au side. They report a magnetic signal appearing at the surface of the Au after a delay comparable to the ballistic transport time of electrons travelling from the Fe layer to the Au surface. Nonetheless what they measure is a more structured signal than what one might have expected. The Au surface first grows a magnetization in opposite direction to the Fe layer and only after 100-200fs the magnetization switches to the expected direction.

The reason to such behaviour is unclear. The explanation that the authors propose neglects the fact that the electrons decrease in energy after scatterings. The sign change can be due to real dynamics of the magnetization or from artefacts of the technique when it is used in such an unusual out-of-equilibrium

situation. As proposed by the authors different spin dependence of transport properties of electrons and holes could lead to such behaviour even if it has to be consistent with the fact that an analogous behaviour is not seen in the ferromagnetic layer or other experiments (so far). Spin superdiffusion can in principle reproduce such a behaviour but that would depend on fine details of the transport properties and such prediction cannot be as reliable as the one showing a very stable behaviour with respect to the material properties.

Demagnetization dynamics in magnetic domain network

More recently two studies showed the effect of spin transport in films arranged with a lateral pattern of antiferromagnetically oriented magnetic domains. In Ref. [48], the authors find a speed up of the demagnetization process. They attribute the phenomenon to the direct spin transfer between neighbouring magnetic domains with antiparallel directions of the magnetization. In Ref. [34] on a similar structure the authors outline that direct spin transfer smoothens the domain wall between neighbouring domains. They have employed superdiffusive spin transport model to describe their findings.

Spin transport in all-optical magnetization switching

In the thesis I have focused only on the dynamics of magnetization in ferromagnets. In ferrimagnets more kinds of dynamics are allowed and their interplay becomes important, but that does not mean that spin superdiffusion is not expected to happen in this kind of materials as well. A very recent work [16] shows that GdFeCo films, usually employed for the all-optical switching, are inhomogeneous and that this inhomogeneity can be the fundamental to the switching. They found that spin transfer happens from Gd poor to Gd rich regions, leading to a switch of the latter. This might be a key mechanism that in turn drives at later times the switching of the whole film.

5. Conclusion and outlook

During my PhD I have proposed the mechanism of superdiffusive spin transport as the driving mechanism of the ultrafast demagnetization and developed the corresponding theoretical model and numerical discretisation [Papers I and II]. Subsequent experimental studies, not only confirmed the mechanism as the driver of, at least, a big fraction of the ultrafast demagnetization, but showed that very strong predictions, like the transfer of magnetic moment in non-magnetic materials [32], the ultrafast increase of magnetization [Paper III] and the ultrafast demagnetization triggered only by the energy dropped by the excited electrons [PaperIV], could be indeed obtained experimentally.

We have also shown that the superdiffusive spin transport model is able to predict with good accuracy the time shape of spin currents and developed a new experimental technique to measure in a contact-less manner such ultrafast magnetization currents [Paper V]. Such study have allowed us to create a first device based on superdiffusive spin currents that can be used as a pulse shaper and as a broadband THz emitter.

These new discoveries have fuelled an already vibrant research field with renewed vitality. The fundamental implication of our findings is that, beside the three-order-of- magnitude increase in magnetic recording speed, the non-local nature of superdiffusive spin transfer opens new horizons for the application of ultrafast magnetization dynamics to information transport technology, where femtosecond spin bunches could be used not only to store information, but also to transport it. The significance of these discoveries goes beyond the idea of ultrafast magnetic recording pointing towards a completely ultrafast spin-electronics.

Nonetheless many open questions remain. It is still not clear whether spin superdiffusion is the only driver of the ultrafast demagnetization. For instance before developing and testing the non-linear behaviour of the model, it is difficult to predict whether the behaviour at high fluence in Paper III can be explained by the material dependence of the saturation of the transport properties, or another process has to be assumed as participating the dynamics. It has also been reported ultrafast demagnetization of a thin metallic film on an insulator substrate. Such geometry should block the spin diffusion towards the substrate, hindering considerably the effectiveness of the superdiffusive spin transport according to the basic scenario proposed. This is currently under investigation.

The plans for the future are to develop a deeper physical understanding of the ultrafast magnetization dynamics on one side and of employing the

knowledge of superdiffusive spin transport to develop proof-of-principle of basic femtospintronics devices.

Svensk sammanfattning

Debatten kring orsaken bakom ultrasnabb avmagnetisering har varit intensiv under de senaste sexton åren. Ett flertal mikroskopiska mekanismer har föreslagits men inga har än så länge tillhandahållit tydliga, obestridliga bevis för sin giltighet. Inom detta sammanhang har jag presenterat ett tillvägagångssätt baserat på spinberoende elektronsuperdiffusion som drivkraft bakom ultrasnabb avmagnetisering.

Exciterade elektroner och hål i den ferromagnetiska metallen sprids efter absorption av laserfotoner. Då materialet är ferromagnetiskt ockuperar majoritets och minoritetsspinkanaler olika band. Därmed är det inte förvånande att materialets transportegenskaper är starkt spinberoende. I de flesta ferromagnetiska metaller har exciterade elektroner av majoritetsspin bättre transportegenskaper än dem av minoritetstyp. Effekten blir att majoritetselektronerna mer effektivt lämnar området bestrålat av lasern vilket leder till spintransport.

Modellering av den ovan beskrivna situationen är inte en trivial uppgift. Transporten kräver en ad hoc beskrivning som tar hänsyn till att både medelfrivägen och livstiden, respektive är i samma storleksordning som systemets dimensioner och effektens tidsrymd. Det kan påvisas att diffusionsregimen varken är standarddiffusion eller ballistisk utan ligger inom området för anomal diffusion och i synnerhet superdiffusion. Vidare genomgår de exciterade elektronerna termalisering medan de sprids vilket påverkar spintransporten. Detta kräver att en komplett Boltzmannbehandling, utan relaxeringstidsapproximationen, tillämpas på transportproblemet.

Nyligen utförda experiment har revolutionerat området genom resultat som visat sig oförenliga med tidigare framställda modeller samt genom att obestridligt påvisa spindiffusion.

Vi har visat att spindiffusionen i riktning från ett lager som genomgår ultrasnabb avmagnetisering kan användas för att skapa en ultrasnabb ökning av magnetisering i ett närliggande magnetiskt lager. Experiment har utförts på ett Ni/Ru/Fe-prov där magnetiska moment hos två magnetiska lager kan drivas till antingen parallell eller antiparallell linjering. Tidsutvecklingen hos två magnetiska moment har mätts oberoende med hjälp av mjuka röntgenpulser. I fallet med antiparallell linjering orsakade spininjektionen en minskning av magnetiseringen i Fe. I fallet med parallell konfigurering observerades istället, för första gången någonsin, en ultrasnabb magnetiseringsökning.

Vidare har vi visat att optiska excitationer inte är en nödvändig förutsättning för ultrasnabb avmagnetisering samt att exciterade elektroner vilka sprids ge-

nom superdiffusion från ett ickemagnetiskt substrat kan ge upphov till avmagnetiseringen. Detta har åstadkommits genom jämförelse av avmagnetiseringsamplituden och tidsformen hos ett typiskt Ni/Al-prov med ett Au/Ni/Al-prov där en del av den optiska pumpen absorberas i Au-lagret. Liknande slutgiltiga avmagnetiseringsamplituder observeras medan Au/Ni/Al-strukturen uppvisar en tidsfördröjning. Orsaken till detta har tillskrivits elektroner som exciteras i Au och sedan sprids till Ni-lagret där de tappar energi och orsakar avmagnetisering.

Slutligen har vi uppvisat möjligheten att kontrollera tidsformen hos de skapade spinströmmarna samt utvecklad en teknik för att direkt uppmäta spinströmmar utan elektriska kontakter. Vi anpassade formen hos magnetiseringsströmmarna genom multilager med lämpligt utvalda material. För att experimentellt bekräfta teoretiska förutsägelser gjordes direkta mätningar av spinströmmar i tre steg: 1) Omvandling av spinström till transversal laddningsström via inversa spin-Hall-effekten, 2) emission av elektromagnetiska fält i Thz-regimen från laddningsströmmen, samt 3) uppmätning av THz-fälten och härledning av strömmarnas form genom inversion av Maxwells ekvationer. Som biprodukt visade vi även att THz-emissionen associerad med processen kommer från transversala elektriska strömmar genererade via inversa spin-Hall-effekten hos de superdiffusiva spinströmmarna.

Påföljden av dessa nya upptäckter går bortom lösningen av mysteriet med ultrasnabb avmagnetisering. Det visar även hur spininformation inte bara kan manipuleras, vilket visats för sexton år sedan, utan framförallt också överföras i oöverträffad fart. Denna upptäckt lägger grunden för komplett femtosekundsspinelektronik.

Acknowledgements

After five years in Uppsala the number of people I should thank is really enormous.

My gratitude goes to Olle Eriksson, who supported me with his wise guidance during the last part of my PhD. In addition to many interesting scientific discussions, he also had the patience to go through my thesis. I am also very grateful to Lars Nordström, for his extremely dense answers to my questions. I wish to thank Peter Oppeneer for inspiring discussions, and for giving me the possibility to develop my ideas.

I am especially grateful to my closest collaborators in Uppsala: Karel Carva, Giuseppe Barbalinardo and Pablo Maldonado. All of them, in their own different ways, both as coworkers and as friends, have made my experience in Uppsala great, really great. It has been a privilege to work with you and to be your friend. A big thank to Dominik Legut; he left not long after I arrived, but he could still drive my first steps with Wien2k, and take me skating on a frozen lake for the first time in my life. Lately I felt very lucky to have had the opportunity to work with Inka Locht, with all her enthusiasm, curiosity and dedication to work. A big thank to Anna Delin for her scientific support in my last project in Uppsala. And last but not least to Raghuveer Chimata who, on top of being a great collaborator, has also been a great company during my lunches at Rullan.

A special thank goes to my dear friend Igor Di Marco. He became my mentor after my arrival in Uppsala; we have had a great time together, we spent a lot of time sharing our views on Sweden, future and life in general and we have spent hours and hours in endless discussions on both important and completely futile topics: it has been really fun, thanks. We have also finally started working on a common project.

There are also other people I have never actively collaborated with, but with whom I have had great scientific discussions. Jan Rusz has been all this time here, always available and helpful, a quiet model of a great scientist and a great person. Patrik Thundström has been a fantastic colleague, one of the nicest people I have ever met and definitely, by far, the most patient one. I have had also great discussions with Johan Hellsvik, Diana Iusan, Oscar Grånäs, Biplab Sanyal, Anders Bergman.

I cannot forget the group of people whit which I have spent uncountable lunches at Rullan or fikas in the kitchen: Vancho, Iulia, Attila, Costas, Sumanta, Beatriz, Adam, Corina, Jonathan, Sara, Ralph, Alex, Manuel, Rodrigo, Mirek, Heike, Satadeep, Dmitry, Saito, Carmine, Lisa, Anna, Nina, Leyla,

Petros, Jonas, Erna, Baotian and many others (oh here I'm definitely forgetting someone...).

I am very grateful to Alex Edström, who helped me hugely with the Swedish summary.

A special mention has to go to the group of the Italians at Ångström and outside: Barbara Brena, Andrea Taroni, Francesco Cricchio, Fabrizio Cossu, Gabriele Tartaglino Mazzucchelli, Stefano Rubino (and Lois and the little Luce Kay, even though they are neither italian nor at Ångström), and Giuseppe Dibitetto, Luca D'Amario, Andrea Palaia and the big Italian group, and Ugo Corte.

A big thank to all the collaborators from other universities. A special thank goes to Markus Münzenberg for the great support and for having involved me in a fantastic project together with another great scientist: Tobias Kampfrath. It has been fun and instructive to work with you. I am grateful to Andrea Eschenlohr and Christian Stamm for all the things I have learned working with you. I wish to thank also all the people involved in the Uppsala-Jülich-Boulder-Kaiserslautern collaboration, Dennis Rudolf, Roman Adam, Claus Schneider, Emrah Turgut, Justin Shaw, Hans Nembach, Tom Silva, Patrik Grychtol, Chan La-O-Vorakiat, Margaret Murnane, Henry Kapteyn, S. Mathias and Martin Aeschlimann. I have received a large amount of interesting and challenging questions from all of you. That helped me a lot to deepen my understanding of ultrafast dynamics. It has definitely been the most instructive project so far.

There are more people with whom I have had the pleasure to interact and who had influenced my scientific development: Sjors Schellekens, Bert Koopmans, Uwe Bovensiepen, Alexey Melnikov, Federico Pressacco, Eduardo Mancini, Christian Back, Marco Finazzi, Matteo Savoini, Sam Khorsand, Andrei Kyrilyuk, Theo Rasing, Hermann Dürr, Jakob Walowski, Boris Ivanov, Andreas Fognini and many others.

Papá, mamma, Ilenia, you are the people who had the greatest influence on who I am today. There is no way to thank you enough for all the unconditioned love and support you have given me.

I will be eternally grateful to Mirja for her existence and for being there for me every day. Everything I have done in my life after meeting you has been thanks to you.

I am sure I have forgotten someone I would have liked to thank. Very many people have had in these years a big or small influence in either my life, my scientific development or both. Sorry if you are not here, blame my bad memory.

References

[1] N. W. Ashcroft and N. D. Mermin. *Solid state physics*. Harcourt College Publishers, 1976.

[2] E. Beaurepaire, J. C. Merle, A. Daunois, and J. Y. Bigot. Ultrafast spin dynamics in ferromagnetic nickel. *Phys. Rev. Lett.*, 76:4250, 1996.

[3] J.-Y. Bigot, M. Vomir, and E. Beaurepaire. Coherent ultrafast magnetism induced by femtosecond laser pulses. *Nat. Phys.*, 5:515, 2009.

[4] S. D. Brorson, J. G. Fujimoto, and E. P. Ippen. Femtosecond electronic heat-transport dynamics in thin gold films. *Phys. Rev. Lett.*, 59:1962, 1987.

[5] E. Carpene, E. Mancini, C. Dallera, M. Brenna, E. Puppin, and S. De Silvestri. Dynamics of electron-magnon interaction and ultrafast demagnetization in thin iron films. *Phys. Rev. B*, 78:174422, 2008.

[6] K. Carva, M. Battiato, and P. M. Oppeneer. Ab Initio Investigation of the Elliott-Yafet Electron-Phonon Mechanism in Laser-Induced Ultrafast Demagnetization. *Phys. Rev. Lett.*, 107:207201, 2011.

[7] K. Carva, M. Battiato, and P. M. Oppeneer. Ab initio theory of electron-phonon mediated ultrafast spin relaxation of laser-excited hot electrons in transition-metal ferromagnets. *Phys. Rev. B*, 87:184425, 2013.

[8] D. Cheskis, A. Porat, L. Szapiro, O. Potashnik, and S. Bar-Ad. Saturation of the ultrafast laser-induced demagnetization in nickel. *Phys. Rev. B*, 72:014437, 2005.

[9] W. T. Coffey, Yu. P. Kalmykov, and J. T. Waldron. *The Langevin equation*. World Scientific, 2004.

[10] F. Dalla Longa, J. T. Kohlhepp, W. J. M. de Jonge, and B. Koopmans. Influence of photon angular momentum on ultrafast demagnetization in nickel. *Phys. Rev. B*, 75:224431, 2007.

[11] S. Essert and H. C. Schneider. Electron-phonon scattering dynamics in ferromagnetic metals and their influence on ultrafast demagnetization processes. *Phys. Rev. B*, 84:224405, 2011.

[12] M. Faehnle and C. Illg. Electron theory of fast and ultrafast dissipative magnetization dynamics. *J. Phys.-Condens. Matter*, 23:493201, 2011.

[13] Manfred Fähnle, Jonas Seib, and Christian Illg. Relating Gilbert damping and ultrafast laser-induced demagnetization. *Phys. Rev. B*, 82:144405, 2010.

[14] W. S. Fann, R. Storz, H. W. K. Tom, and J. Bokor. Direct measurement of nonequilibrium electron-energy distributions in subpicosecond laser-heated gold-films. *Phys. Rev. Lett.*, 68:2834, 1992.

[15] W. S. Fann, R. Storz, H. W. K. Tom, and J. Bokor. Electron thermalization in gold. *Phys. Rev. B*, 46:13592, 1992.

[16] C. E. Graves, A. H. Reid, T. Wang, B. Wu, S. de Jong, K. Vahaplar, I. Radu, D. P. Bernstein, M. Messerschmidt, L. M/"uller, R. Coffee, M. Bionta, S. W. Epp, R. Hartmann, N. Kimmel, G. Hauser, A. Hartmann, P. Holl, H. Gorke,

J. H. Mentink, A. Tsukamoto, A. Fognini, J. J. Turner, W. F. Schlotter, D. Rolles, H. Soltau, L. Str/"uder, Y. Acremann, A. V. Kimel, A. Kirilyuk, Th. Rasing, J. St/"ohr, A. O. Scherz, and H. A. D/"urr. Nanoscale spin reversal by non-local angular momentum transfer following ultrafast laser excitation in ferrimagnetic GdFeCo. *Nat. Mater.*, 12:293, 2013.

[17] J. Hohlfeld, E. Matthias, R. Knorren, and K. H. Bennemann. Nonequilibrium Magnetization Dynamics of Nickel. *Phys. Rev. Lett.*, 78:4861, 1997.

[18] T. Juhasz, H. E. Elsayed-Ali, G. O. Smith, C. Suárez, and W. E. Bron. Direct measurements of the transport of nonequilibrium electrons in gold films with different crystal structures. *Phys. Rev. B*, 48:15488, 1993.

[19] A. R. Khorsand, M. Savoini, A. Kirilyuk, and Th. Rasing. *comment under review in Nat. Mater.*

[20] A. Kirilyuk, A. V. Kimel, and T. Rasing. Ultrafast optical manipulation of magnetic order. *Rev. Mod. Phys.*, 82:2731, 2010.

[21] B. Koopmans, H. H. J. E. Kicken, M. van Kampen, and W. J. M. de Jonge. Microscopic model for femtosecond magnetization dynamics. *J. Magn. Magn. Mater.*, 286:271, 2005.

[22] B. Koopmans, G. Malinowski, F. Dalla Longa, D. Steiauf, M. Faehnle, T. Roth, M. Cinchetti, and M. Aeschlimann. Explaining the paradoxical diversity of ultrafast laser-induced demagnetization. *Nat. Mater.*, 9:259, 2010.

[23] B. Koopmans, J. J. M. Ruigrok, F. D. Longa, and W. J. M. de Jonge. Unifying ultrafast magnetization dynamics. *Phys. Rev. Lett.*, 95:267207, 2005.

[24] B Koopmans, M van Kampen, JT Kohlhepp, and WJM de Jonge. Ultrafast magneto-optics in nickel: Magnetism or optics? *Phys. Rev. Lett.*, 85:844, 2000.

[25] M. Krauss, T. Roth, S. Alebrand, D. Steil, M. Cinchetti, M. Aeschlimann, and H. C. Schneider. Ultrafast demagnetization of ferromagnetic transition metals: The role of the Coulomb interaction. *Phys. Rev. B*, 80:180407(R), 2009.

[26] R. Kubo. Statistical-mechanical theory of irreversible processes. 1. general theory and simple applications to magnetic and conduction problems. *J. Phys. Soc. Jpn*, 12:570, 1957.

[27] C. La-O-Vorakiat, M. Siemens, M.M. Murnane, H.C. Kapteyn, S. Mathias, M. Aeschlimann, P. Grychtol, R. Adam, C.M. Schneider, J.M. Shaw, H. Nembach, and T. J. Silva. Ultrafast demagnetization dynamics at the M edges of magnetic elements observed using a tabletop high-harmonic soft x-ray source. *Phys. Rev. Lett.*, 103:257402, 2009.

[28] C. La-O-Vorakiat, E. Turgut, C.A. Teale, H.C. Kapteyn, M.M. Murnane, S. Mathias, M Aeschlimann, C.M. Schneider, and J.M. Shaw. Ultrafast Demagnetization Measurements Using Extreme Ultraviolet Light: Comparison of Electronic and Magnetic Contributions. *Phys. Rev. X*, 2:011005, 2012.

[29] G. Malinowski, F. Dalla Longa, J. H. H. Rietjens, P. V. Paluskar, R. Huijink, H. J. M. Swagten, and B. Koopmans. Control of speed and efficiency of ultrafast demagnetization by direct transfer of spin angular momentum. *Nat. Phys.*, 4:855, 2008.

[30] L. Mandel and E. Wolf. *Optical coherence and quantum optics*. Cambridge University Press, 1995.

[31] S. Mathias, C. La-O-Vorakiat, P. Grychtol, P. Granitzka, E. Turgut, J. M. Shaw, R. Adam, H. T. Nembach, M. E. Siemens, S. Eich, C. M. Schneider, T. J. Silva,

M. Aeschlimann, M. M. Murnane, and H. C. Kapteyn. Probing the timescale of the exchange interaction in a ferromagnetic alloy. *PNAS*, 109:4792, 2012.
[32] A. Melnikov, I. Razdolski, T. O. Wehling, E. Th. Papaioannou, V. Roddatis, P. Fumagalli, O. Aktsipetrov, A. I. Lichtenstein, and U. Bovensiepen. Ultrafast Transport of Laser-Excited Spin-Polarized Carriers in Au/Fe/MgO(001). *Phys. Rev. Lett.*, 107:076601, 2011.
[33] G. M. Müller, J. Walowski, M. Djordjevic, G.-X. Miao, A. Gupta, A. V. Ramos, K. Gehrke, V. Moshnyaga, K. Samwer, J. Schmalhorst, A. Thomas, A. Hütten, G. Reiss, J. S. Moodera, and M. Münzenberg. Spin polarization in half-metals probed by femtosecond spin excitation. *Nat. Mater.*, 8:56, 2009.
[34] B. Pfau, S. Schaffert, L. Müller, C. Gutt, A. Al-Shemmary, F. Büttner, R. Delaunay, S. Düsterer, S. Flewett, R. Frömter, J. Geilhufe, E. Guehrs, C. M. Günther, R. Hawaldar, M. Hille, N. Jaouen, A. Kobs, K. Li, J. Mohanty, H. Redlin, W. F. Schlotter, D. Stickler, R. Treusch, B. Vodungbo, M Kläui, H. P. Oepen, J. Lüning, G. Grübel, and S. Eisebitt. Ultrafast optical demagnetization manipulates nanoscale spin structure in domain walls. *Nat. Commun.*, 3:1100, 2012.
[35] I. Radu, G. Woltersdorf, M. Kiessling, A. Melnikov, U. Bovensiepen, J.-U. Thiele, and C. H. Back. Laser-Induced Magnetization Dynamics of Lanthanide-Doped Permalloy Thin Films. *Phys. Rev. Lett.*, 102:117201, 2009.
[36] H. Regensburger, R. Vollmer, and J. Kirschner. Time-resolved magnetization-induced second-harmonic generation from the Ni(110) surface. *Phys. Rev. B*, 61:14716, 2000.
[37] E. Saitoh, M. Ueda, H. Miyajima, and G. Tatara. Conversion of spin current into charge current at room temperature: inverse spin-Hall effect. *Appl. Phys. Lett.*, 88:182509, 2006.
[38] A. J. Schellekens and B. Koopmans. private communication.
[39] A. Scholl, L. Baumgarten, R. Jacquemin, and W. Eberhardt. Ultrafast Spin Dynamics of Ferromagnetic Thin Films Observed by fs Spin-Resolved Two-Photon Photoemission. *Phys. Rev. Lett.*, 79:5146, 1997.
[40] M. S. Si and G. P. Zhang. Resolving photon-shortage mystery in femtosecond magnetism. *J. Phys.-Condens. Matter*, 22:076005, 2010.
[41] C. Stamm, T. Kachel, N. Pontius, R. Mitzner, T. Quast, K. Holldack, S. Khan, C. Lupulescu, E. F. Aziz, M. Wietstruk, H. A. Durr, and W. Eberhardt. Femtosecond modification of electron localization and transfer of angular momentum in nickel. *Nat. Mat.*, 6:740, 2007.
[42] C. Stamm, N. Pontius, T. Kachel, M. Wietstruk, and H. A. Duerr. Femtosecond x-ray absorption spectroscopy of spin and orbital angular momentum in photoexcited ni films during ultrafast demagnetization. *Phys. Rev. B*, 81:104425, 2010.
[43] C. D. Stanciu, F. Hansteen, A. V. Kimel, A. Kirilyuk, A. Tsukamoto, A. Itoh, and Th. Rasing. All-optical magnetic recording with circularly polarized light. *Phys. Rev. Lett.*, 99:047601, 2007.
[44] D. Steiauf and M. Faehnle. Elliott-Yafet mechanism and the discussion of femtosecond magnetization dynamics. *Phys. Rev. B*, 79:140401(R), 2009.
[45] C. K. Sun, F. Vallee, L. H. Acioli, E. P. Ippen, and J. G. Fujimoto. Femtosecond-tunable measurement of electron thermalization in gold. *Phys.*

Rev. B, 50:15337, 1994.
[46] M.-L. Théye. Investigation of the optical properties of Au by means of thin semitransparent films. *Phys. Rev. B*, 2:3060, 1970.
[47] I. Tudosa, C. Stamm, A. B. Kashuba, F. King, H. C. Siegmann, J. Stöhr, G. Ju, B. Lu, and D. Weller. The ultimate speed of magnetic switching in granular recording media. *Nature*, 428:831, 2004.
[48] B. Vodungbo, J. Gautier, G. Lambert, A. B. Sardinha, M. Lozano, S. Sebban, M. Ducousso, W. Boutu, K. Li, B. Tudu, M. Tortarolo, R. Hawaldar, R. Delaunay, V. López-Flores, J. Arabski, C. Boeglin, H. Merdji, P. Zeitoun, and J. Lüning. Laser-induced ultrafast demagnetization in the presence of a nanoscale magnetic domain network. *Nat. Commun.*, 3:999, 2012.
[49] J. Walowski, G. Müller, M. Djordjevic, M. Münzenberg, M. Kläui, C. A. F. Vaz, and J. A. C. Bland. Energy Equilibration Processes of Electrons, Magnons, and Phonons at the Femtosecond Time Scale. *Phys. Rev. Lett.*, 101:237401, 2008.
[50] A. Weber, F. Pressacco, S. Günther, E. Mancini, P. M. Oppeneer, and C. H. Back. Ultrafast demagnetization dynamics of thin Fe/W(110) films: Comparison of time- and spin-resolved photoemission with time-resolved magneto-optic experiments. *Phys. Rev. B*, 84:132412, 2011.
[51] M. Wietstruk, A. Melnikov, C. Stamm, T. Kachel, N. Pontius, M. Sultan, C. Gahl, M. Weinelt, H. A. Duerr, and U. Bovensiepen. Hot-Electron-Driven Enhancement of Spin-Lattice Coupling in Gd and Tb 4f Ferromagnets Observed by Femtosecond X-Ray Magnetic Circular Dichroism. *Phys. Rev. Lett.*, 106:127401, 2011.
[52] G. P. Zhang and W. Hübner. Laser-induced ultrafast demagnetization in ferromagnetic metals. *Phys. Rev. Lett.*, 85:3025, 2000.
[53] V. P. Zhukov, E. V. Chulkov, and P. M. Echenique. GW+T theory of excited electron lifetimes in metals. *Phys. Rev. B*, 72:155109, 2005.
[54] V. P. Zhukov, E. V. Chulkov, and P. M. Echenique. Lifetimes and inelastic mean free path of low-energy excited electrons in Fe, Ni, Pt, and au: Ab initio GW+T calculations. *Phys. Rev. B*, 73:125105, 2006.

Acta Universitatis Upsaliensis

Digital Comprehensive Summaries of Uppsala Dissertations from the Faculty of Science and Technology 1061

Editor: The Dean of the Faculty of Science and Technology

A doctoral dissertation from the Faculty of Science and Technology, Uppsala University, is usually a summary of a number of papers. A few copies of the complete dissertation are kept at major Swedish research libraries, while the summary alone is distributed internationally through the series Digital Comprehensive Summaries of Uppsala Dissertations from the Faculty of Science and Technology.

Distribution: publications.uu.se
urn:nbn:se:uu:diva-205265

ACTA
UNIVERSITATIS
UPSALIENSIS
UPPSALA
2013